DECEMBER 1972

MDC G4401

ELECTRODES FOR THERMIONIC CONVERTERS

PHASE II-III FINAL REPORT

by
J. G. DeSteese

Prepared under Contract No. 953125 by
Donald W. Douglas Laboratories
McDonnell Douglas Astronautics Company
for
JET PROPULSION LABORATORY

PREFACE

This document is the Phase II and III final report submitted by the Donald W. Douglas Laboratories, a subdivision of the McDonnell Douglas Astronautics Company, Richland, Washington, under Contract No. 953125 and covers the period from 16 April 1972 through 8 December 1972.

This program was monitored by the Jet Propulsion Laboratory, Pasadena, California, for the National Aeronautics and Space Administration; Dr. K. Shimada was the Technical Monitor.

This work was performed for the Jet Propulsion Laboratory, California Institute of Technology, sponsored by the National Aeronautics and Space Administration under Contract NAS7-100.

CONTENTS

FIGURES

SUMMARY

The JPL metal/ceramic Marchuk tube was reconstructed in Phase II and successfully operated with a quiescent cesium vapor plasma corresponding to cesium liquid reservoir temperatures from 376° to 427°K. The work function characteristics of tantalum test emitters coated with anodic oxide films 1 to 118 nm thick were measured to evaluate the applicability of the materials as the collector surface in a plasma-mode thermionic converter. Work function minima between 1.4 and 1.5 ev were observed. The effect of electronegative surface layers was partially obscured by additive vapor impurities detected by the clean tantalum reference emitter.

The anodic films were dissolved in the tantalum substrate of the test emitters which were used to check performance of the oxygen-doped tantalum in the emitter regime of conventional plasma-mode thermionic converters. The results generally corroborated Phase I data showing an increase in effective bare work function with oxygen doping. Work function decay corresponding to oxygen loss from all doped specimens was observed during operation at 1900° to 1950°K for 160 hours.

The Phase III program evaluated 2% thoriated tungsten as an emitter material in the conventional converter. Thoriated tungsten activated at 1800°K exhibited a transition from a ϕ_0 of 3.4 to 3.5 ev on the cesium-bare plateau to a characteristic approximating that of clean tungsten in the obsorption regime. After operation at higher temperatures (to 2400°K), the thorium supply was depleted and the entire characteristic tended towards that of clean tungsten. Transient surface conditions were inferred from work function data which suggested that both electropositive and electronegative additives were diffused to the active surface.

The conventional glass Marchuk tube proved more convenient and reliable than the metal/ceramic version.

Section 1
INTRODUCTION

In the past decade, a major goal in cesium-vapor thermionic converters has been the development of electrodes which have favorable work functions in cesium at the lowest possible vapor pressure. Reduced cesium pressure tends to minimize the irreversible vapor conduction loss component in the emitter thermal balance. In cesium-plasma converters, the product of cesium pressure (p) and electrode spacing (d) is an important parameter in the determination of optimum converter performance. A reduction in cesium pressure can be accompanied by larger, and therefore, more practical electrode spacings while maintaining the pd product in the optimum range.

The principal approach to modifying converter electrode surfaces has been selecting and treating materials to provide a cesiated work function characteristic which occurs at high surface-to-cesium-reservoir temperature ratios (T/T_{Cs}) on the Rasor-Warner diagram (Reference 1). The Phase I Final Report (Reference 2) provides examples of surface modification techniques reported in the literature. In general, surface modifications may be classified in two categories:

1. Surface orientation to expose high bare-work-function crystal structure.
2. Exposure of cesiated surfaces to electronegative additives.

In practical devices, it is important that electrode treatment be stable throughout the operating lifetime of the converter. Electrodes with the longest potential life appear to be supplied by additives which may be replenished from a reservoir to compensate for removal of the adsorbate from the active surface. Two such surface systems which appear worthy of further study are Ta-O-Cs and W-Th-Cs. The beneficial additive effect obtained by dissolution of oxygen in cesiated tantalum has been recognized for some time and has shown long-term stable electrode operation in the ISOMITE® battery development program (Reference 3). The oxygen component in the Ta-O-Cs surface system can be supplied from a substrate of bulk Ta-O solid solution. Although its major application so

far has been in relatively low temperature devices (emitter temperature, $T_e < 1400°K$), it appears potentially useful as both an emitter and collector material in conventional plasma-mode converters.

A recent study at JPL indicated a high bare-work-function characteristic of thoriated tungsten used in a test converter. In this surface system, the electrode is prepared from 0.5% to 2% distribution of thoria in tungsten. The thoria is partially reduced to metallic thorium by high-temperature activation (Reference 4). Metallic thorium formed in the interior of the electrode diffuses along grain boundaries and forms a monatonic film on the surface. Both oxygenated tantalum and thoriated tungsten, therefore, are candidate materials which dispense the surface additive from the bulk material of the electrode. The Phase II and Phase III programs study, respectively, thermionic emission characteristics of Ta-O and W-Th surface systems.

PROGRAM OBJECTIVES

The objective of the Phase II effort was to measure the cesiated work function of tantalum test emitters coated with anodic oxide films of various thicknesses. A goal of this effort was to evaluate the material as a candidate collector for plasma-mode thermionic converters and was complementary to the Phase I study which investigated the application of oxygen-doped tantalum as an emitter material. A further objective of Phase II was conversion of anodically-coated tantalum to oxygen-doped material to corroborate and amplify results of the Phase I study.

The Phase III objective was to determine the cesiated work function characteristics of 2% thoriated tungsten and measure the effect of operating at temperatures above 1800°K.

PROGRAM STRUCTURE

Work function measurements of all materials involved the use of wire-loop test emitters exposed to cesium vapor in a Marchuk-type plasma-anode tube (Reference 5). Phase I and II studies were performed with a JPL-supplied metal/ceramic tube. Phase III effort was accomplished using a conventional glass plasma-anode tube constructed at DWDL.

Phase II consisted of six principal tasks:

Task 1 - Fabricate three tantalum test electrodes.

Task 2 - Fabricate one tantalum reference electrode.

Task 3 - Prepare Marchuk plasma-anode tube, install test emitters, and cesiate assembly.

Task 4 - Measure low temperature (<1200°K) emission characteristics of cesiated test emitters with anodic films intact.

Task 5 - Measure high temperature (1250° to 2400°K) emission characteristics of cesiated test emitters in the range $2.0<T/T_{Cs}<4.8$.

Task 6 - Operate test emitters at the lowest temperature between 1700° and 2000°K which yields measurable electron emission for ~150 hr to determine initial stability of oxygen doping.

Phase III effort consisted of five principal tasks:

Task 1 - Fabricate two 2% thoriated tungsten test emitters.

Task 2 - Fabricate one tungsten reference test emitter.

Task 3 - Construct glass Marchuk tube, install test emitters, and cesiate assembly.

Task 4 - Measure emission characteristics of test emitters in the range $2.0<T/T_{Cs}<5.0$ at surface temperatures to 1800°K.

Task 5 - Repeat emission measurements for test emitters after operation at temperatures to 2400°K.

The following sections describe experimental techniques used to accomplish these tasks, and results and recommendations derived from the Phase II and Phase III programs.

Section 2
EXPERIMENTAL APPROACH

The Phase II experimental approach was based on using a JPL-supplied metal/ceramic Marchuk tube which had been operated previously with argon by Shimada and Cassell (Reference 6). Difficulties were experienced with this tube in the Phase I program (Reference 2) and therefore, several modifications were introduced to improve the quality of emission measurements in cesium vapor.

Tantalum-wire test emitters coated with anodic oxide films from 1 to 118 nm thick were prepared and mounted in the Marchuk tube. Thermionic emission measurements were made in cesium vapor and compared with emission characteristics of a rigorously outgassed but untreated tantalum reference electrode. Conditions corresponding to the collector regime in a conventional cesium plasma converter were investigated. Dissolution of the anodic films in preoxygenated tantalum substrates permitted an approximate duplication of the nominal 0.1, 0.2, and 0.3 atomic percent (a/o) oxygen-doped specimens studied in Phase I. Emission characteristics of oxygen-doped emitters were measured under conditions appropriate for emitter operation in a conventional converter.

In all experiments with the metal/ceramic Marchuk tube, the cesium source was provided by an external refluxing cesium still. The system imcorporated a Vac-Ion high-vacuum system which continuously pumped the Marchuk tube through an orifice plate to prevent excessive loss of cesium vapor.

To facilitate concurrent Phase III studies, the thoriated-tungsten study was performed in a conventional Marchuk tube with a glass envelope. Cesium was vacuum-distilled from a glass ampoule and sealed in the tube after appropriate processing. Emission measurements of thoriated tungsten were made in cesium vapor and compared with characteristics of the rigorously outgassed tungsten reference electrode. The effect of operating one thoriated-tungsten emitter at temperatures to 2400°K was observed by comparing its emission properties with those of the tungsten reference electrode and the second thoriated-tungsten emitter.

This section contains a detailed summary of construction and preparation techniques used in the Phase II and Phase III efforts.

PHASE II PROGRAM

Preparatory Material Processing

As in Phase I, four certified-purity (Appendix A) 0.254-mm (10-mil) diameter tantalum wires were ultrasonically cleaned in reagent-grade ethyl alcohol, suspended in a Vac-Ion high vacuum system, and outgassed to provide a reference condition prior to oxygen doping. Wire samples approximately 30-cm long were outgassed sequentially for 1 hour between 2400° and 2500°K. After each high-temperature run, a residual 1.33×10^{-7} N/m^2 (1×10^{-9} torr) pressure was indicated by the Vac-Ion pump current. Each wire was flashed several times and accumulated approximately 10 minutes at 2800°K.

Wire temperature was measured by an Epic micropyrometer which was calibrated using an NBS-traceable standard with corrections for bell jar transmissivity. Correlation between brightness temperature and true temperature was derived from thermal emissivity data in Reference 4. Further details of this procedure are described in Reference 2.

Anodization of Tantalum

A literature survey was performed (Reference 2) which indicated aqueous anodization as the preferred techniqued for producing oxide films on tantalum. Anodization was performed in a glass measuring cylinder 30 cm long as shown in Figure 2-1. The tantalum wire to be anodized was suspended on the axis of symmetry, and connected to the positive terminal of a power supply. The wire was kept under slight tension by a previously anodized tantalum weight. Tantalum foil formed into a cylinder was placed inside the glass and connected to the negative side of the power supply through a four-terminal current shunt. Voltages proportional to cell current and voltage were indicated on a recorder. The space between electrodes was filled with a 0.01 molar HNO_3 solution at 293°K. Anodization was achieved with a 1-ma/cm^2 current density, and film thickness was inferred from cell voltage.

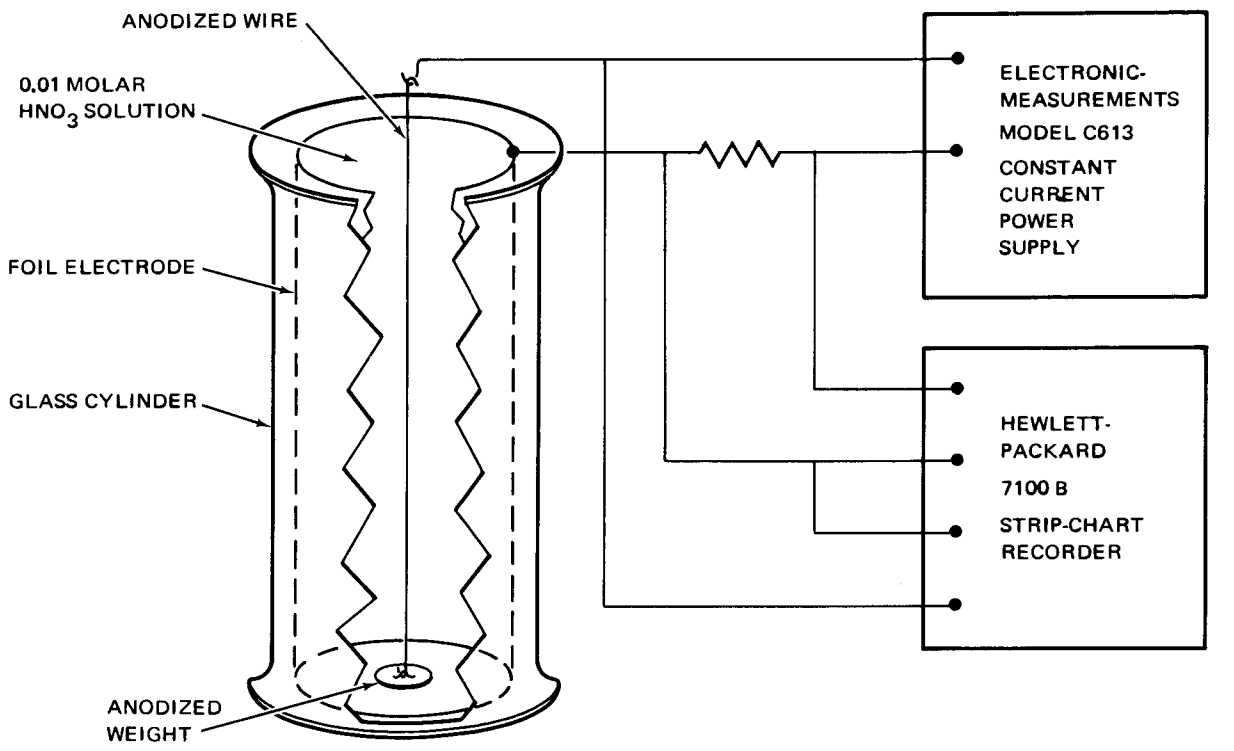

Figure 2-1. Anodization Method

The theory summarized in the Phase I final report (Reference 2) shows that the rate of change in anodic film thickness with cell voltage (dx/dv) is given by

$$\frac{dx}{dv} = \frac{1}{\frac{1}{\beta}\ln\frac{J_{ox}}{\alpha}} \qquad (2\text{-}1)$$

where J_{ox} is the ionic current density; α and β are tantalum oxidation constants.

Using values for α and β determined by Vermilyea (Reference 7) for oxidation in aqueous media,

$$\frac{dx}{dv} = 1.56 \text{ nm/v} \qquad (2\text{-}2)$$

Because the results of Phase I were compromised by noisy plasma and leakage conditions, an attempt was made to corroborate and amplify Phase I results by designing the Phase II test emitters to serve two purposes. Material for the

test emitters was first anodized and the oxygen film dissolved in the substrate to provide some oxygen predoping. The wires were returned to the anodization cell where additional anodization was performed until film thickness required for the Phase II study were obtained. Table 2-1 summarizes anodic film thicknesses and doping levels for the three specimens.

To accommodate a rerun of Phase I and the Phase II experiment, small compromises were made in both doping level and film thickness, In the Phase I experiment, a 0.2 a/o oxygen doping required a 118-nm anodic film (Reference 2).

A wire anodized to 118 nm thickness was prepared to represent the nominal 100-nm film thickness of the third Phase II specimen. The 1- and 10-nm specimens for Phase II were respectively prepared by secondary anodization of Phase I specimens predoped to the 0.1 and 0.3 a/o level. After completion of Phase II studies and dissolution of the second anodic film layer, the final oxygen doping level used for rerun of Phase I duplicated the original Phase I preparation to within 2% for the 0.1 a/o sample and 6% for the 0.3 a/o specimen. The deviation from the nominal film thickness of the 100-nm Phase II specimen amounted to 18%; as in all cases, the purpose of the experiment was to establish order-of-magnitude effects, the compromises summarized in Table 2-1 were considered acceptable and, with the exception of the 100-nm film, within the overall uncertainty band of the Marchuk measuring technique.

Test Emitter Construction (Tasks 1 and 2)

Four emitters were constructed from the central portion of the processed wires; one was made from each anodized sample and one from the rigorously outgassed

Table 2-1

ANODIC FILM THICKNESS AND DOPING LEVEL

Phase II Required Film Thickness (nm)	Phase I Required Oxygen Doping (a/o)	Phase I Required Film Thickness (nm)	Phase II Additional Film Thickness (nm)	Phase I Rerun Final Oxygen Doping (a/o)
1	0.1	59	1	0.102
10	0.3	177	10	0.317
100	0.2	118	0	0.200

material. To avoid any material that had not been properly outgassed, sections 5 cm from the ends were discarded. Figure 2-2 shows a typical emitter mounted on a Varian flange. Nickel leads were connected to the ends of the test emitter loop and shielded by nesting ceramic tubes to within 1.5 cm of the flange. Two guard rings protecting the junction of the ceramics were connected to a third nickel lead. The nickel leads were brazed into Alberox type CT-250 metal/ceramic leadthrough assemblies. Ceramic sleeves on each emitter were fired in a 10^{-4} N/m^2 ($\sim 10^{-6}$ torr) vacuum at 1800°K for one hour before assembly.

The exposed length of each emitter was determined to the required accuracy (±2.5%) by measuring the loop length on a >10x enlarged photograph. Copper wires were bent to conform to the enlarged probe image and knife edge witness marks were made at the points of emergence from the ceramic sleeves. The copper wires were straightened and the distance between marks measured with a vernier caliper. The scale of the photograph was determined by the ratio of the apparent diameter to the actual diameter measured with a precision micrometer. Maximum error contributed by this method was 0.25 mm in the length of the enlarged photograph. This corresponds to approximately 0.03 mm error in estimating the actual loop length. A greater uncertainty was contributed by possible plasma penetration into the bore of the ceramic sleeves. An additional 1 mm, a distance equal to the bore diameter, was added to the measured loop length to account for plasma penetration. This contributed a ±2% uncertainty in estimating the superficial electron emission area.

Two modifications in probe design were made to promote a better signal/noise ratio in the emitter circuit. As shown in Figure 2-2, a ceramic disc was added at the base of the long ceramic sleeves to inhibit plasma leakage into the test emitter port. The length of the exposed loop of each specimen was also reduced to approximately 1.3 cm to halve the magnitude of the positive ion current collected by the cold emitter. For comparison, the test emitter configuration used in the Phase I experiment is shown in Figure 2-5 of the Phase I final report (Reference 2). Table 2-2 summarizes Phase II test emitter exposed superficial length and area.

Preparation of Marchuk Tube (Task 3)

At the end of the Phase I experiment, the cesium still was cooled and the Marchuk tube and connecting tubulation heated to expel any remaining cesium. After the tube was baked 24 hr at ~500°K, the cesium still was valved off and the Marchuk tube cooled to room temperature. Disassembly of the tube revealed considerable corrosion effects of cesium on the Alberox leadthrough assemblies.

Corrosion products in the form of fine grit-like deposits (Figure 2-3) has fallen onto the ceramic tube liner from the downward facing ports. Tantalum straps and the anode plate showed evidence of gettering residual gas during the experiment. Initially outgassed bright metallic tantalum appeared to have blue and gray oxide surface films after exposure. Discoloration of the ceramic liner in the tube was also apparent (Figure 2-4).

All components of the tube envelope were ultrasonically cleaned in one Alconox and distilled water solution, three distilled water rinses, and one rinse of reagent-grade ethyl alcohol. Components were dried with a hot air gun. The ceramic tube liner was air baked at 1300°K for 12 hours. All Alberox leadthrough assemblies were helium leak checked after cleaning. One was not leaktight and was discarded. Additional contamination trapped in the crevices of the other Alberox insulator assemblies was ejected by ultrasonic irrigation in Alconox solution.

The tantalum cathode assembly was modified as shown in Figure 2-5. The spiral filament of the Phase I experiment was replaced with tantalum ribbon to reduce voltage across the cathode. In Phase I, the cathode spiral required 6 volts to establish an adequate emission current. This voltage caused local discharges for T_{Cs} >470°K and extreme instability in the main plasma. The ribbon cathode was outgassed prior to assembly and reached an adequate emitter temperature at only 3 volts.

The Marchuk tube assembly was mounted on all metal bakeable valves and reconnected to the DWDL cesium still, residual gas analyzer (RGA), and associated vacuum system as described in the Phase I final report (Reference 2). Heater tapes and an insulation jacket were installed. The Marchuk tube was leak checked and baked between 520° and 620°K until the minimum residual pressure was achieved. As previously observed in the Phase I experiment, pressures less

2355

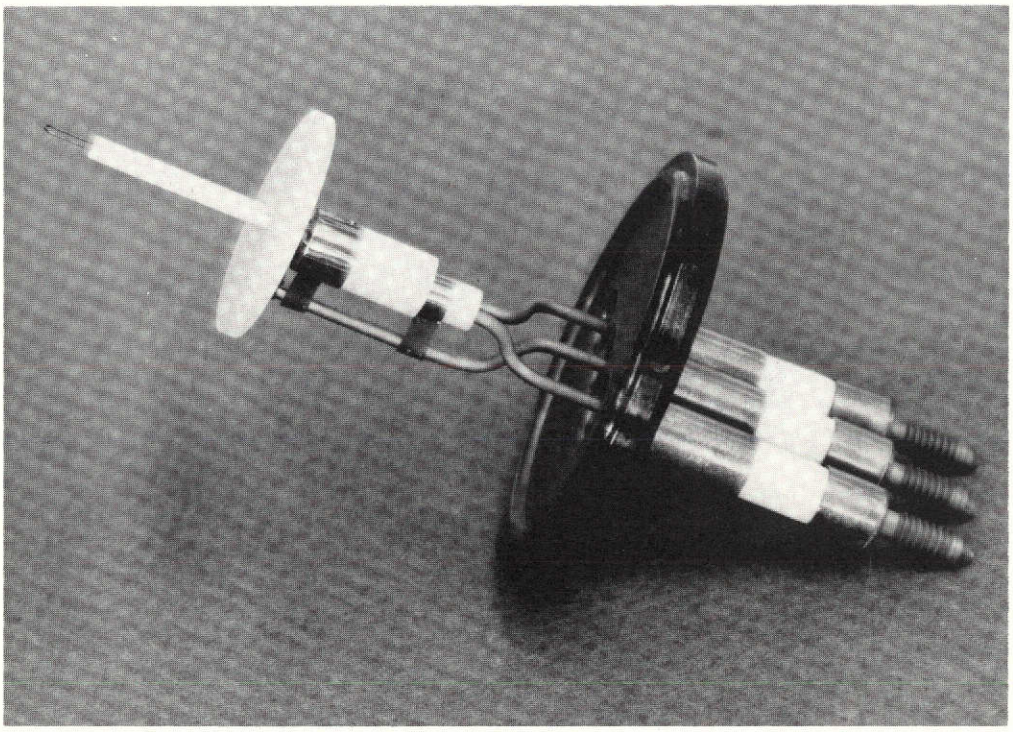

Figure 2-2. Improved Test Emitter Configuration

2300

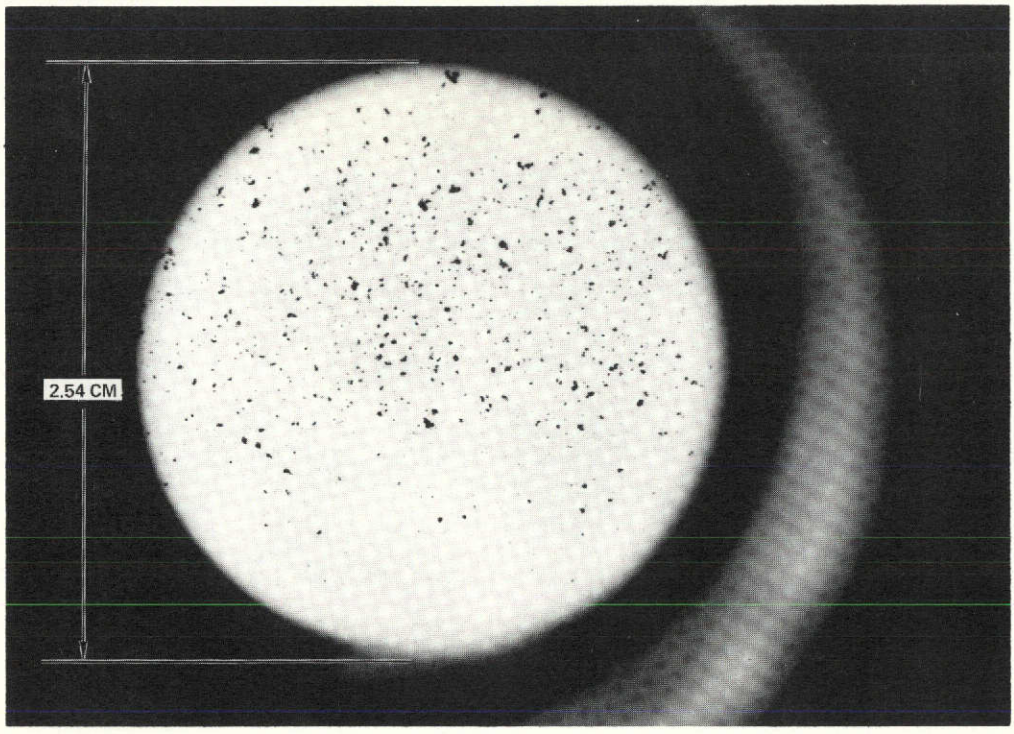

Figure 2-3. Particle Deposit Under Downward-Facing Emitter Port

2305

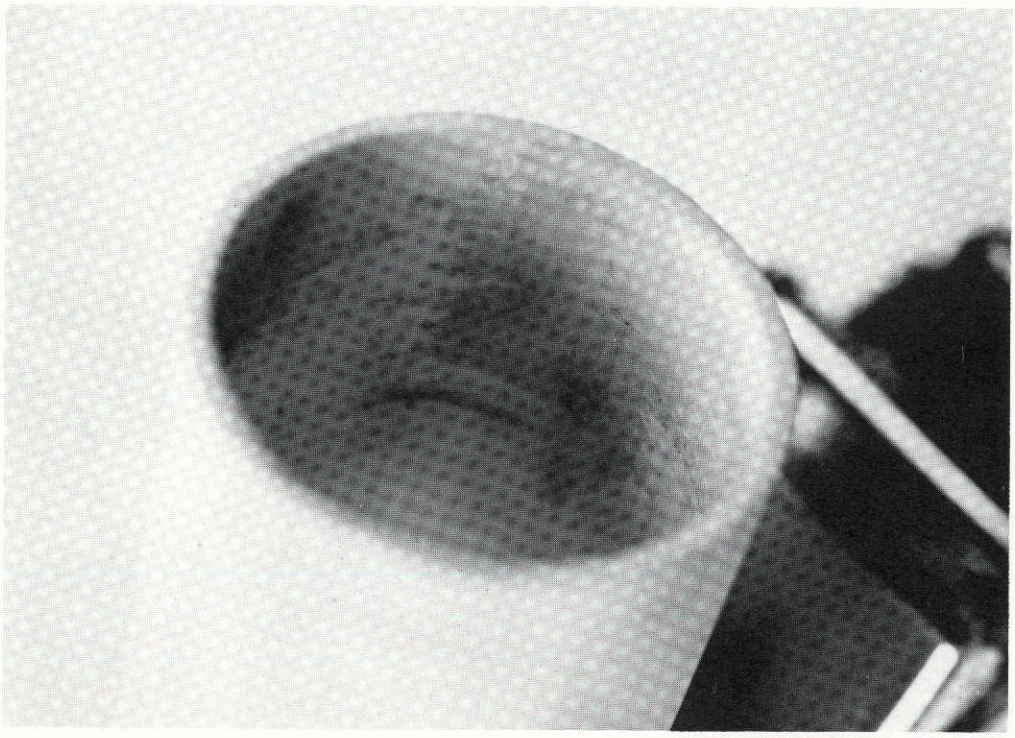

Figure 2-4. Discoloration on Ceramic Tube Liner

2357

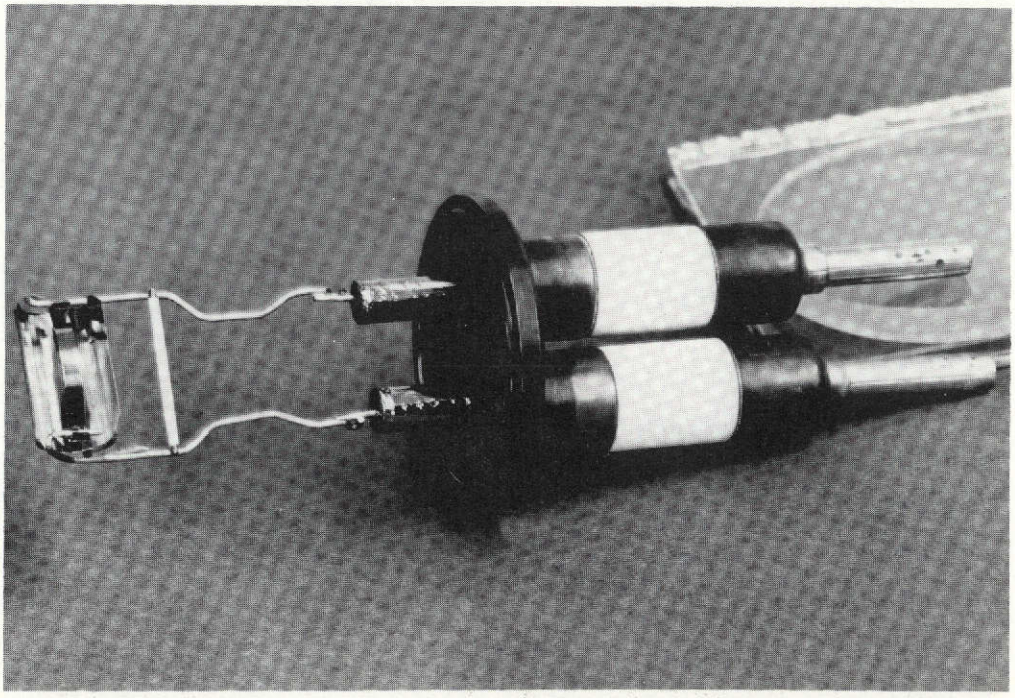

Figure 2-5. Tantalum Ribbon Cathode

Table 2-2

PHASE II TEST EMITTER SUPERFICIAL EXPOSED LENGTH AND AREA

Emitter No.	Phase II Film Thickness (nm)	Exposed Superficial Length (cm)	Exposed Superficial Area (cm^2)
1	1	1.292	0.103
2	10	1.342	0.107
3	118	1.232	0.098
4	Ref	1.217	0.097

than 10^{-5} N/m^2 ($\sim 10^{-7}$ torr) and 10^{-7} N/m^2 ($\sim 10^{-9}$ torr) were achieved at 620° and 295°K, respectively. The refurbished Marchuk tube operated without failure during Phase II and the rerun of the Phase I program.

Marchuk Tube Measuring Circuit

Figure 2-6 shows changes made in the measuring circuit to improve the Phase II signal/noise ratio in the test emitter circuit. As is standard practice with the Marchuk experiment, test emitters were heated with halfwave-rectified current and emission currents were measured during the off-half cycle to prevent disturbance of the signal by the heating current. A detailed description of the measuring circuit is included in the Phase I final report (Reference 2). The Phase II circuit contained two principal changes. Test emitter bias was provided by a Hewlett-Packard Harrison dc power supply connected with its negative terminal to the grounded side of the cathode. A Superior Electric Company line voltage regulator was added to the circuit to stabilize the cathode and test emitter power supplies. Grounding of the cathode was incorporated to extinguish spurious discharges which occurred during Phase I experiments between the floating cathode and the grounded Marchuk tube body. Grounding of the Marchuk tube body is unavoidable as a result of its connection to the still, vacuum system, and RGA. The test emitter selector switch was modified to include a fifth position as shown in Figure 2-7. The switch provided appropriate connections for test emitter power, bias voltage, and guard rings. The open position permitted series-connection of the test probes for the doping stability test rerun on Phase I work. In all other respects, the measuring circuit is the same as the circuit developed in the Phase I program (Reference 2).

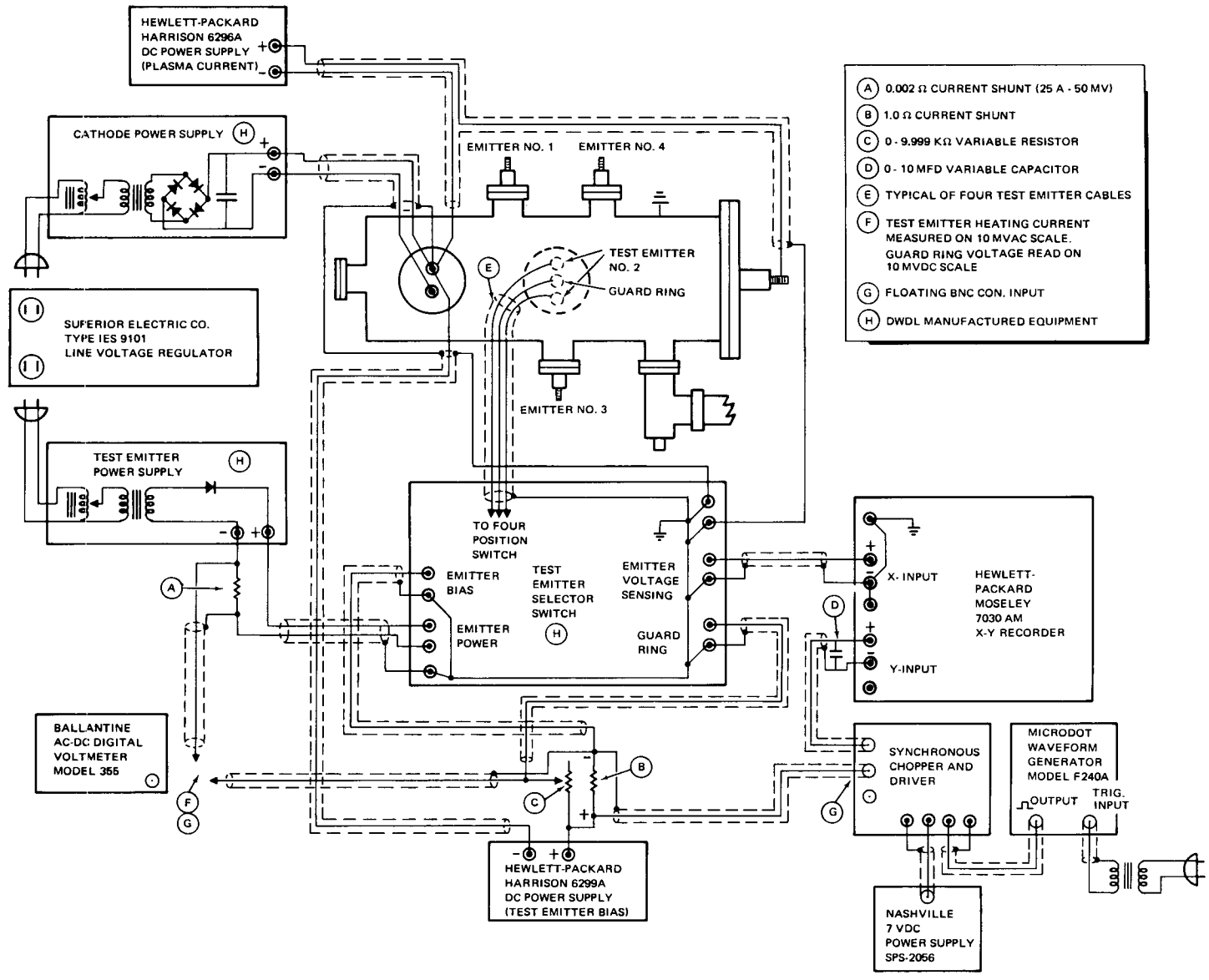

Figure 2-6. Revised Measuring Circuit

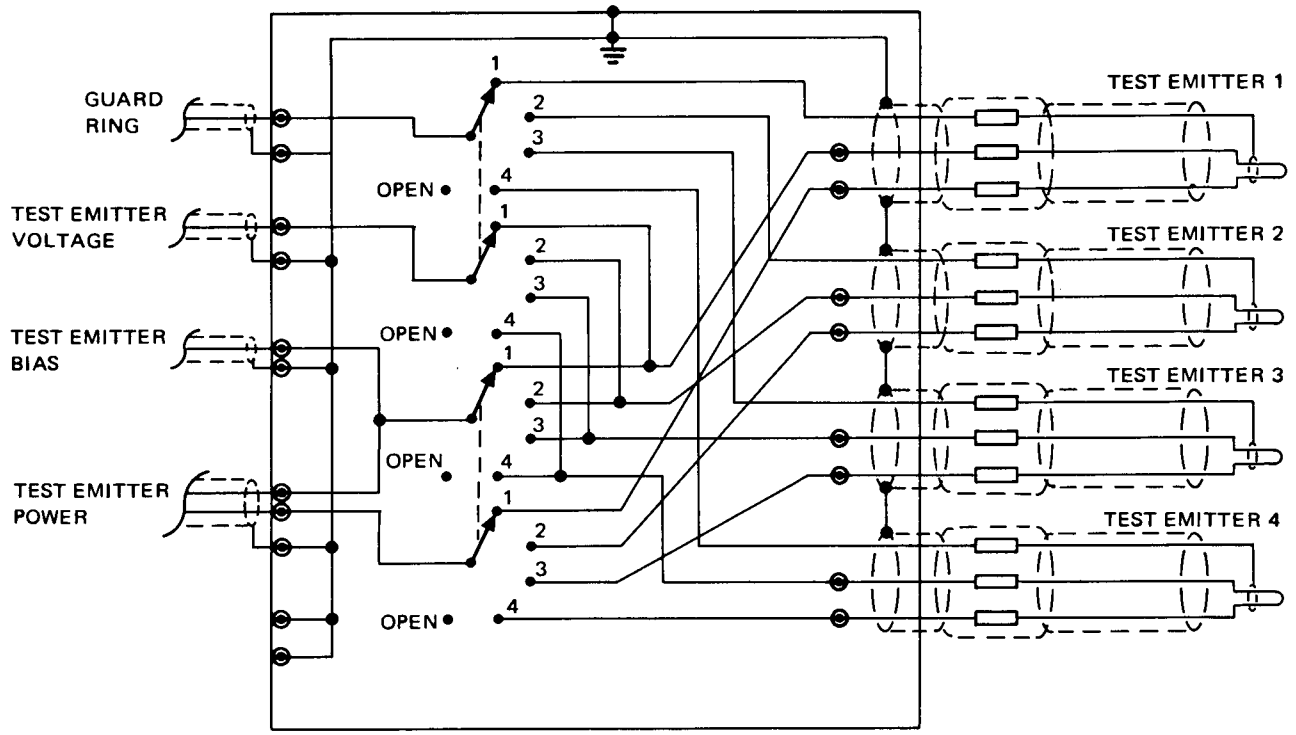

Figure 2-7. Test Emitter Selector Switch Circuit

Test Procedure (Tasks 4 and 5)

The Marchuk tube was heated to an average of 10°K above the cesium reservoir temperature in the still. Additional heat was added to regions such as leadthrough flanges and valves where cesium condensation was possible or apparent. Temperature calibrations were made as a function of heater current on duplicate specimens mounted in a bell jar as shown in Figure 2-8. The temperature of all specimens was measured from 293° and 2400°K. The low-temperature calibration (<1200°K) was based on a correlation between heating current and specimen resistivity. The high-temperature calibration was achieved by a correlation between heating current and pyrometer readings. Discrimination of resistivity and emissivity effects caused by the presence of anodic films and bulk doping were accomplished. A full description of the low-temperature calibration effort performed under separage JPL contract is reported in References 8 and 9. All temperature calibrations involving the Epic micropyrometer were referenced to a NBS-traceable standard with corrections for viewport transmissivity. Tantalum thermal emissivity data were taken from Reference 4 to calculate true emitter temperatures.

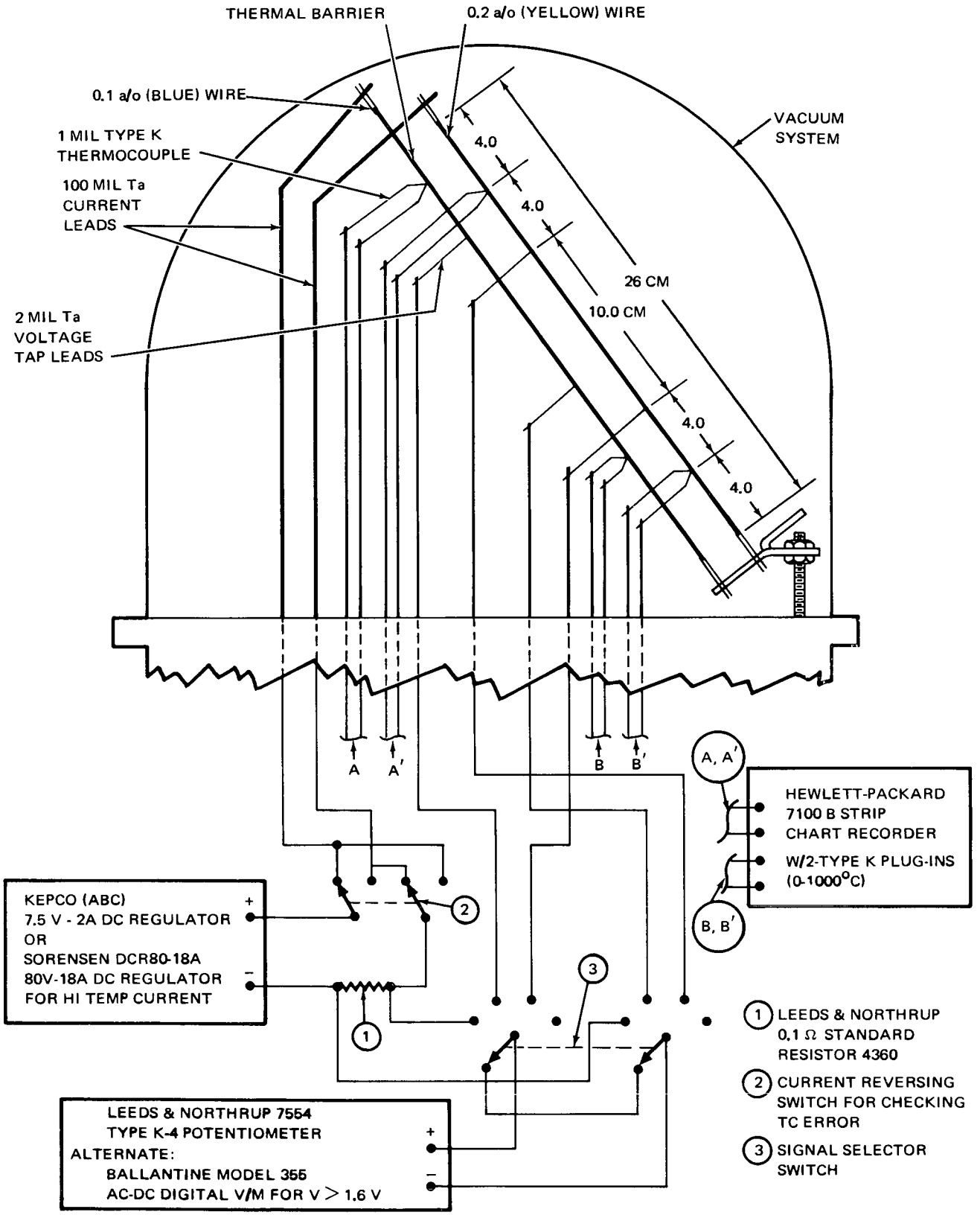

Figure 2-8. Experimental Arrangement for Temperature Calibration

Cesium was admitted from the still with T_{Cs} in the range 382° to 432°K. Cesium reservoir temperatures in excess of 432°K could not be investigated because unstable plasma conditions were generated in the Marchuk tube. Typical operating conditions of the main discharge were an anode/cathode potential difference of 30 volts and discharge current between 50 and 250 ma. With each emitter at Marchuk-tube temperature, a plot of emitter current as a function of bias potential was made to indicate positive ion current from the plasma. Each emitter was then heated, in turn, and emission characteristics were recorded over various temperature ranges. Initial investigation was for $293° < T < 700°K$ at appropriate cesium pressures to scan the range $1.0 < T/T_{Cs} < 2.5$ with all anodic films intact. This procedure was repeated by increasing the upper temperature limit by intervals of 100° until 1200°K was attained. With 1200°K, cesium still conditions were changed to investigate the range $2.0 < T/T_{Cs} < 4.8$.

The procedure described in Phase I final report was used to diffuse anodic films into the tantalum substrate and so produce oxygen-doping approximating the same as that achieved in the Phase I effort. Emission characteristics to 2400°K were than obtained to generate complete ϕ vs T/T_{Cs} curves. Above 1300°K, emitter temperatures were measured with the plasma extinguished to check the calibration derived previously from wires in the bell jar. The procedure was devised to achieve reliable emission measurements with the minimum loss of oxygen at high temperatures. All temperature calibration data were correlated with a digital voltage analog of the emitter heater current. Calibration checks throughout the experiment showed repeatability to ±20°K at all temperatures.

Test Procedure (Task 6)

A 160-hr life test of doping effects was performed in the temperature range from 1900° to 1950°K. For this test, the emitter selector switches were turned to position 5 and four emitters were connected electrically in series and heated by a common current. Conventional emission measurements were separately performed, at intervals, on each emitter.

Test emitter work functions were calculated from the following derivative of the Richardson-Dushman equation,

$$\phi = -kT \ln \frac{J}{A_R T^2} \qquad (2\text{-}3)$$

where

ϕ is work function (ev)
$k = 8.62 \times 10^{-5}$ ev/°K
T is emitter temperature (°K)
J is emission current density (amp/cm^2)
A_R is the Richardson constant (120 amp/cm^2 · °K)

Calculated work functions were plotted as functions of the emitter-temperature-to-cesium-reservoir-temperature (T/T_{Cs}) ratio, as described by Rasor and Warner (Reference 1).

After emission measurements and the doping stability test were completed, cesium was condensed into the still, the tube was baked out, sealed under vacuum, and demounted from the system. The metal/ceramic Marchuk tube assembly was sent to JPL in a condition suitable for further experimentation.

PHASE III PROGRAM

Preparatory Material Processing

Tungsten and thoriated-tungsten wire samples, ceramic sleeves, and all tube components were ultrasonically cleaned in Alconox solution, distilled water, and grain alcohol. Ceramic components were baked in a 6.5×10^{-4} N/m^2 ($\sim 5 \times 10^{-6}$ torr) vacuum at 1650°K for approximately 1 hr. Further processing of the test emitter loop material was performed in place in the assembled tube, to avoid difficulties of forming highly outgassed tungsten wire.

Test Emitter Construction (Tasks 1 and 2)

Two test emitters were constructed from certified-purity (Appendix B) 0.254-mm (10-mil) diameter 2% thoriated-tungsten wire. A third test emitter was constructed from high purity (Appendix C) tungsten wire of the same

diameter. Test emitters were mounted on three-lead glass presses received from Glass Instruments, Inc. Figure 2-9 shows general emitter construction details. Tungsten wire was aligned inside ceramic sleeves by tantalum bushings. Nickel foil provided a spot-weld interface between the tantalum and tungsten. This subassembly was connected by tantalum extension legs to two tungsten leadthroughs in the glass press. Nesting ceramic tubes protected the bushing and extension-lead region of the emitter assembly. A tantalum foil cap protected the junction of the nesting tubes and was connected to a Ta extension of the third leadthrough. A spring wiper of tungsten foil was attached to the guard ring lead and arranged to wipe a platinum bright surface painted on the inside of the test emitter port. Test emitter components are shown in Figure 2-10.

Sufficient tungsten wire protruded into the ceramic sleeves to isolate the exposed loop from thermal conduction effects of the leadthroughs. Test emitters were heated in a bell jar by electric current and observed with the Epic pyrometer. In the incandescent temperature range, no difference in temperature greater than the resolving power of the instrument.

Emitter superficial area was determined as for the Phase I and Phase II effort. A 1-mm allowance for plasma penetration into the bore of the ceramic sleeves was added to the measured area. Table 2-3 summarizes the Phase III test emitter exposed superficial length and area.

Table 2-3

PHASE II TEST EMITTER SUPERFICIAL EXPOSED LENGTH AND AREA

Emitter No.	Emitter Material	Exposed Superficial Length (cm)	Exposed Superficial Area (cm^2)
1 W	W	1.005	0.080
2 W	W-2%ThO_2	1.159	0.094
3 W	W-2%ThO_2	1.052	0.086

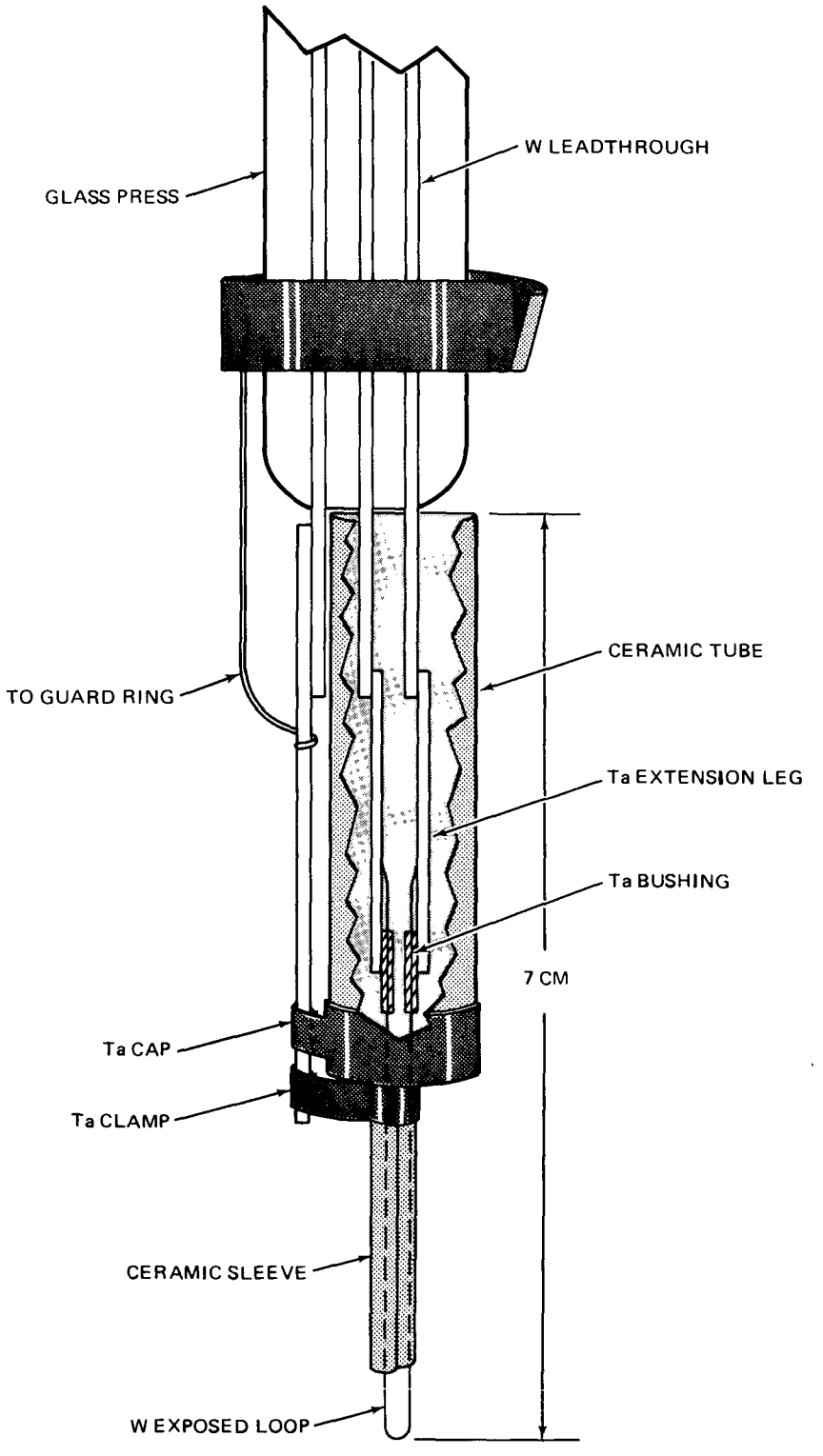

Figure 2-9. Test Emitter Construction for Glass Envelope

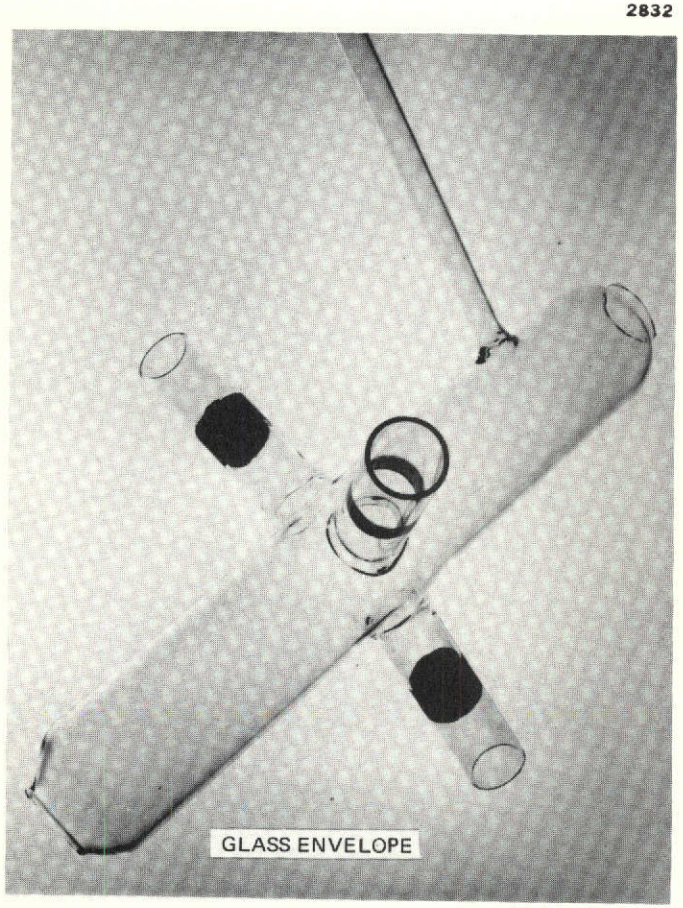

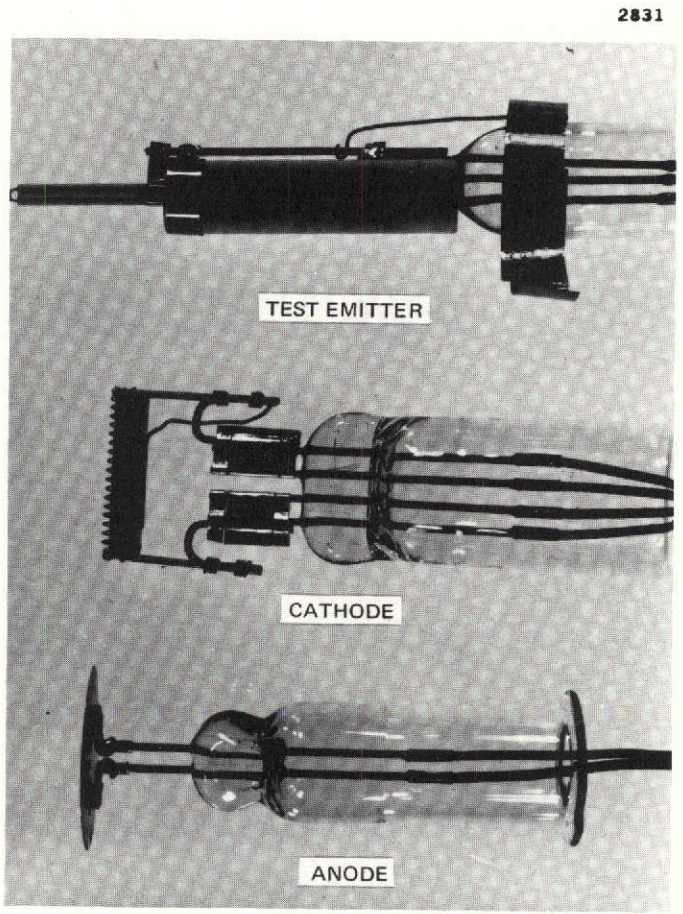

Figure 2-10. Glass Marchuk Tube Components

Construction of Marchuk Tube (Task 3)

Components of the glass Marchuk-tube are shown in Figure 2-10. A glass envelope was made from 51-mm diameter Pyrex Type 7740 tubing, Glass Instruments, Inc. presses with tungsten leadthroughs, and uranium glass transitions were sealed into the envelope. The anode was formed by a tungsten disc 2.7 cm in diameter. The cathode spiral and shield were tungsten mounted on tantalum current leads. A four-lead press was used with the cathode, with two leads ganged for each polarity to share the current load. A platinum bright guard ring was painted on each of three test emitter side arms. The configuration of the side arms permitted the test emitters to enter the plasma at essentially the same potential. The side arms were arranged around the tube at 120° intervals. Emitters were positioned with the loops within 0.5 cm of the tube axis of symmetry. This close proximity was considered desirable and permitted one tungsten and one thoriated-tungsten test emitter to act as a detector of material vaporized from the third emitter.

The assembled Marchuk tube was connected by a U-shaped cold trap to a Vac-Ion high vacuum system with a 270 l/s pumping capability. A high-purity ampoule of cesium metal (Kawecki Chemical Company, Lot No. 1079) was placed in the side arm with a magnetic breaker. The tube was pumped down and baked for 24 hr at 650°K. During this time, the thoriated tungsten emitters were heated several hours at ~1800°K to establish some degree of aging as determined by the constancy of pyrometer readings referred to heater current. The cathode was outgassed for 8 hours at temperatures in excess of normal operation. The tungsten reference emitter was aged at 2400°K until a constant heating current calibration was obtained and then it was flashed to 2800°K for a total of 100 seconds.

After baking the tube, a temperature calibration was made for each test emitter. As described previously, the Epic micropyrometer was used with a calibration reference to a NBS-traceable standard, with corrections for the transmissivity of the glass envelope. Emissivity data corrolating observed and true temperature were derived from Reference 4. In the absence of data in the literature, the emissivity of thoriated-tungsten specimens was taken to be the same as that of pure tungsten. This appears to be an acceptable

assumption considering the expectancy that thorium on the surface, is present at less than a monolayer. As the principal range of interest was in the incandescent temperature regime, no extrapolation of pyrometer readings was made into the non-incandescent range.

The cesium ampoule was broken under a vacuum of 10^{-6} N/m^2 ($<10^{-8}$ torr) and was distilled into the Marchuk tube with a liquid nitrogen cold trap between the tube and vacuum station (Figure 2-11). The tube was sealed at this residual pressure with ~0.2 gram of cesium in the envelope.

Marchuk Tube Measuring Circuit

The measuring circuit of the glass Marchuk tube was nearly identical to that of the Phase II experiment. The two differences were the presence of only three test emitters and the replacement of the test emitter selector switch with a barrier strip. In all other respects, the circuits were identical.

2701-1

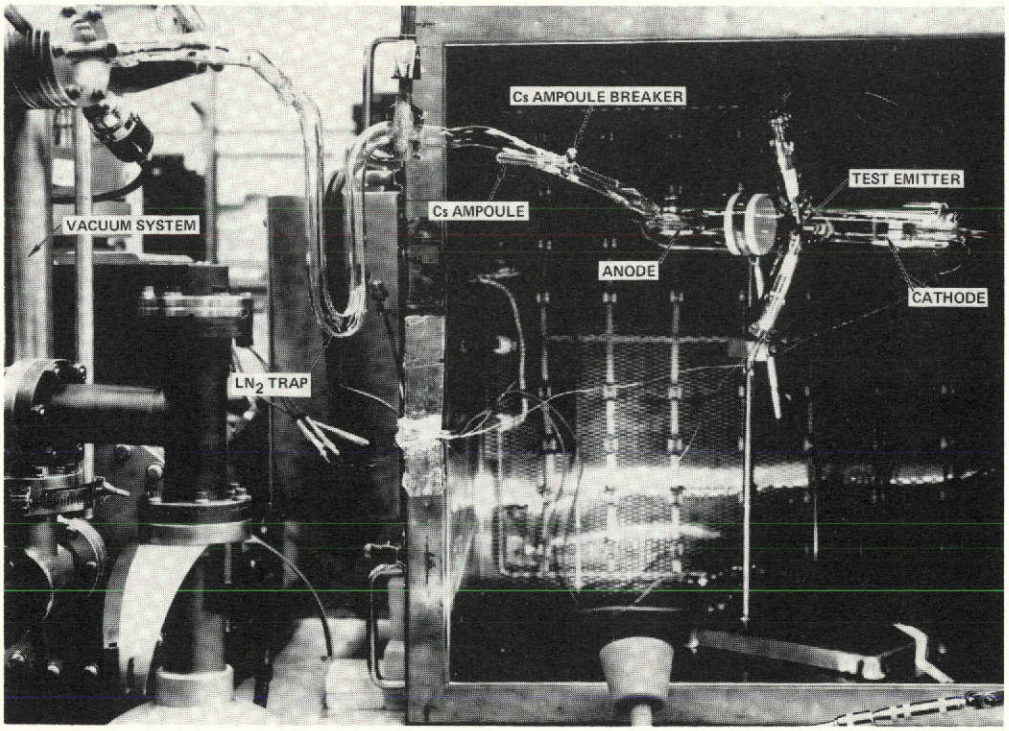

Figure 2-11. Glass Marchuk Tube and Vacuum Connection

Test Procedure (Task 4)

The Marchuk tube was heated in an air oven, thermostatically controlled to within ±2°K. The Marchuk tube was instrumented with five thermocouples placed to anticipate cold spots. Thermocouple readings were displayed on a strip-chart recorder and the lowest was taken as the effective reservoir temperature. The uncertainty in measuring T_{Cs} was ±2°K.

Thermionic emission from thoriated-tungsten test emitters was measured at temperatures to 1800°K with the cesium reservoir temperatures from 376° to 427°K. For each temperature, work function was calculated and plotted on ϕ vs T/T_{Cs} diagrams. Similar data were generated by the W reference emitter to 2400°K.

After significant portions of the adsorption and bare work function region had been scanned, the temperature calibration of each emitter was checked with the tube at room temperature and in the absence of a discharge. The calibration of the thoriated-tungsten emitters was increased incrementally to 2400°K. Between each calibration, a new set of emission data were collected. During this experiment, test emitter No. 3W showed evidence of thorium depletion. Thereafter, maximum operating temperature range was extended to 2400°K while that of emitter No. 2W was held at the 2000°K level. The tungsten reference and 2W emitters were used as detectors of surface-vaporized species from test emitter No. 3W. Final surface conditions and characteristics of each emitter were determined by running each at the highest temperature of its previous calibration for 1 hr to observe the relative constancy of emission characteristics.

After emission measurements were completed the tube was disassembled and the test emitters sent to JPL for further analysis.

Section 3

EXPERIMENTAL RESULTS

The Phase II and Phase III experiments provided unambiguous emission data on anodized and oxygen-doped tantalum and tungsten and thoriated-tungsten species. These results are discussed in this section.

PHASE II RESULTS

Work Function Measurements (Tasks 4 and 5)

A typical emission current vs bias potential plot is shown in Figure 3-1. A significant improvement is evident in the resolution of emission current corresponding to emitter temperatures in the range 1300° to 1950°K, compared with that measured in the Phase I effort. Data from Tasks 4 and 5 are summarized in Figure 3-2 through 3-5. For the anodized samples, runs 1 through 4 present data with anodic films totally or partially intact. Subsequent runs were taken to high temperatures to establish the influence of oxygen-doping on the substrate bare work function. Probe No. 4 (Figure 3-5) was operated over the full temperature range in all runs to identify effects which may have resulted from arrival of additive vapors from the plasma.

Good agreement between the Phase I and Phase II results was obtained in the bare work function region of the tantalum reference electrode. Previously measured $\phi_0 = 4.38 \pm 0.05$ ev was reproduced in the Phase II experiment. Phase II scatter in the adsorption region of the ϕ vs T/T_{Cs} characteristic was generally reduced, and the indicated adsorption characteristic was parallel to the calculated curve. The last Run No. 7 shows a significant shift to the right of the diagram. These data and points below 3 ev probably result from adsorption of additives supplied by the plasma. Most probable candidates are oxygen or oxide species released from the other test emitters and/or other components of the metal/ceramic assembly. If Run No. 7 is ignored, the general tendency in the regime $2 \phi 2.5$ and $2 < T/T_{Cs} 3$ is for the tantalum reference emitter to appear as a surface with $\phi_0 \sim 4.8$ ev, in contradiction to the indication of the plateau region of the curve.

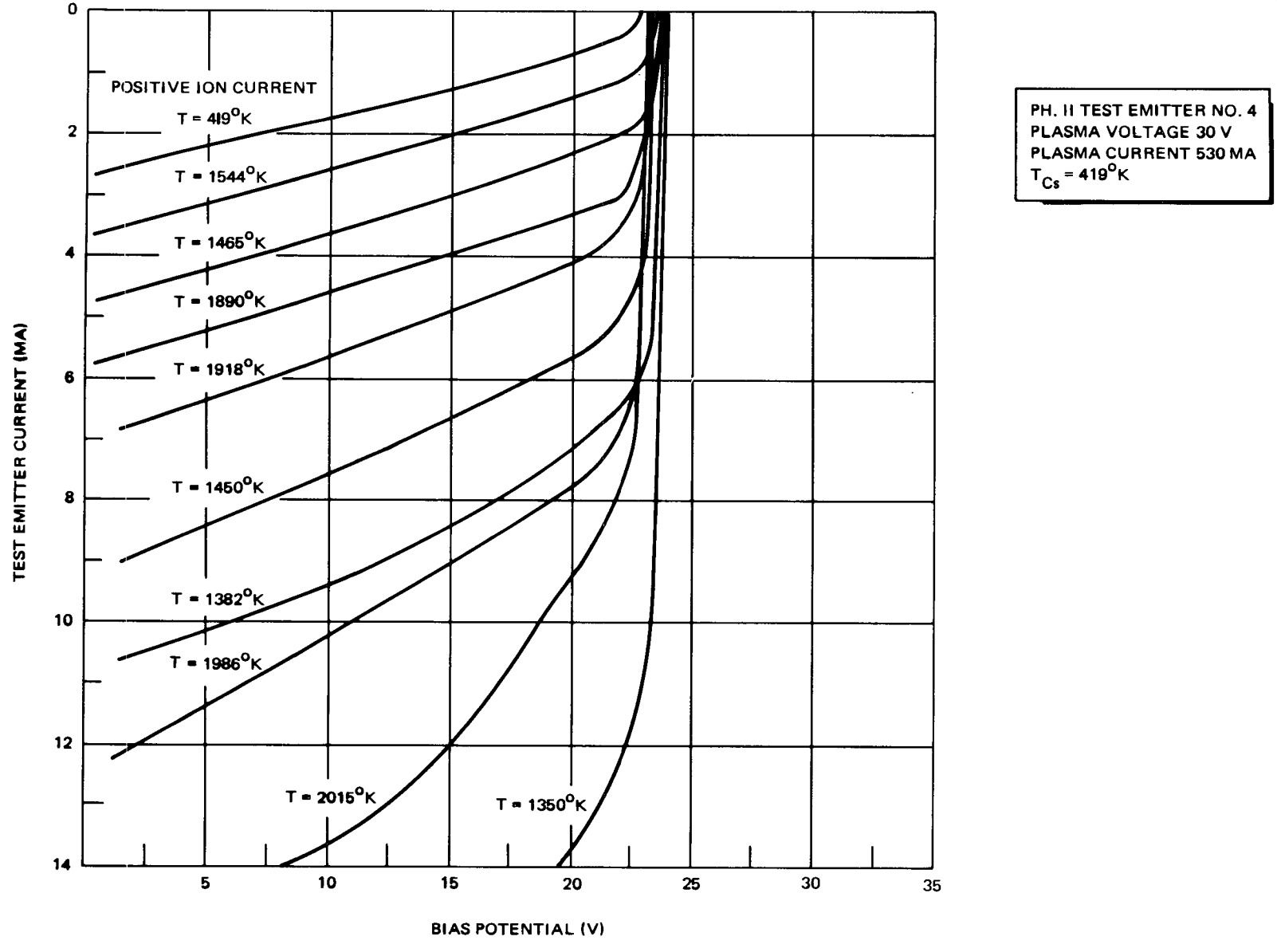

Figure 3-1. Typical Emitter Current vs Bias Potential Measured in Phase II and Phase III Effort

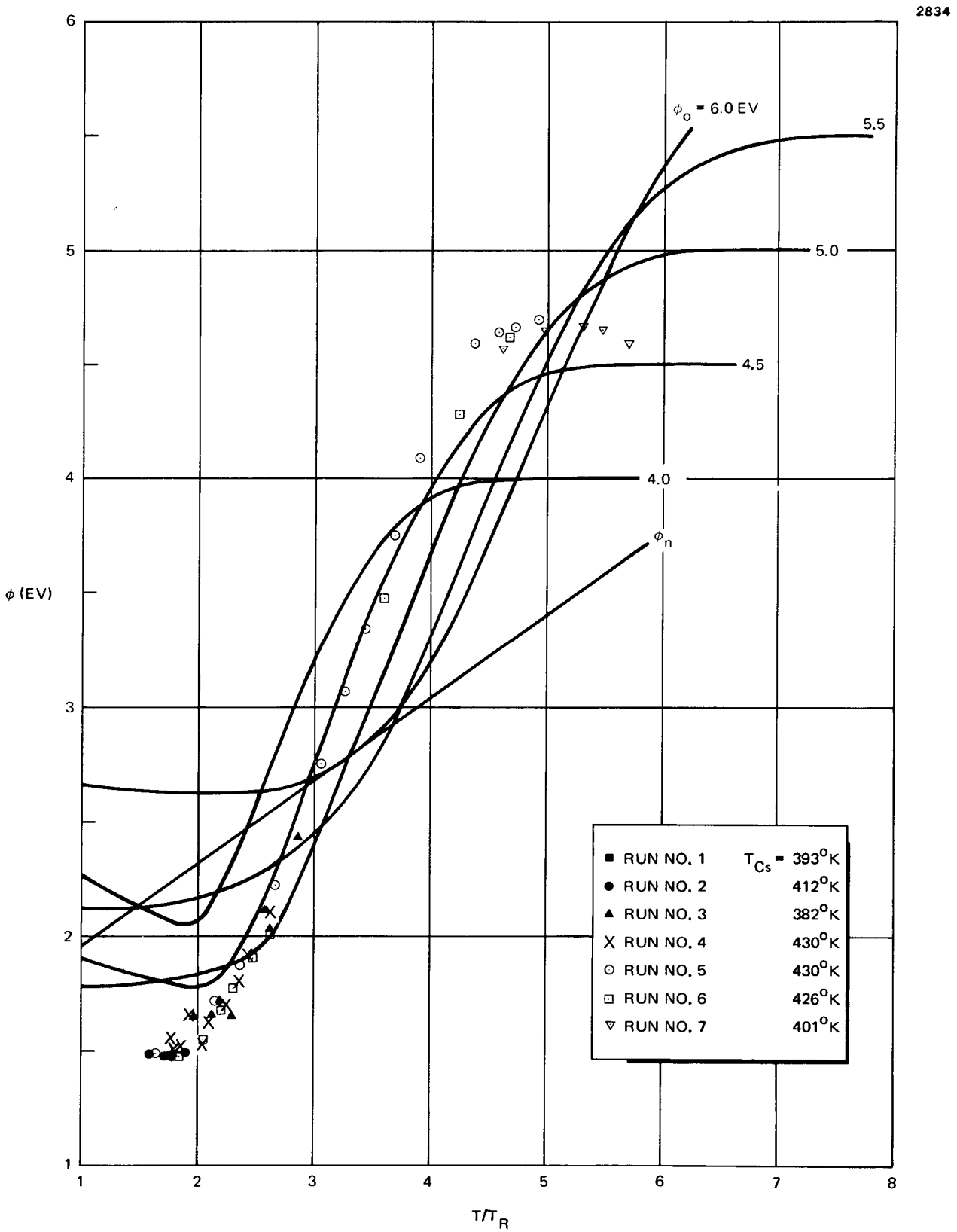

Figure 3-2. ϕ vs T/T_{Cs} Test Emitter No. 1 (1 nm anodic film; ~0.1 a/o oxygen doping)

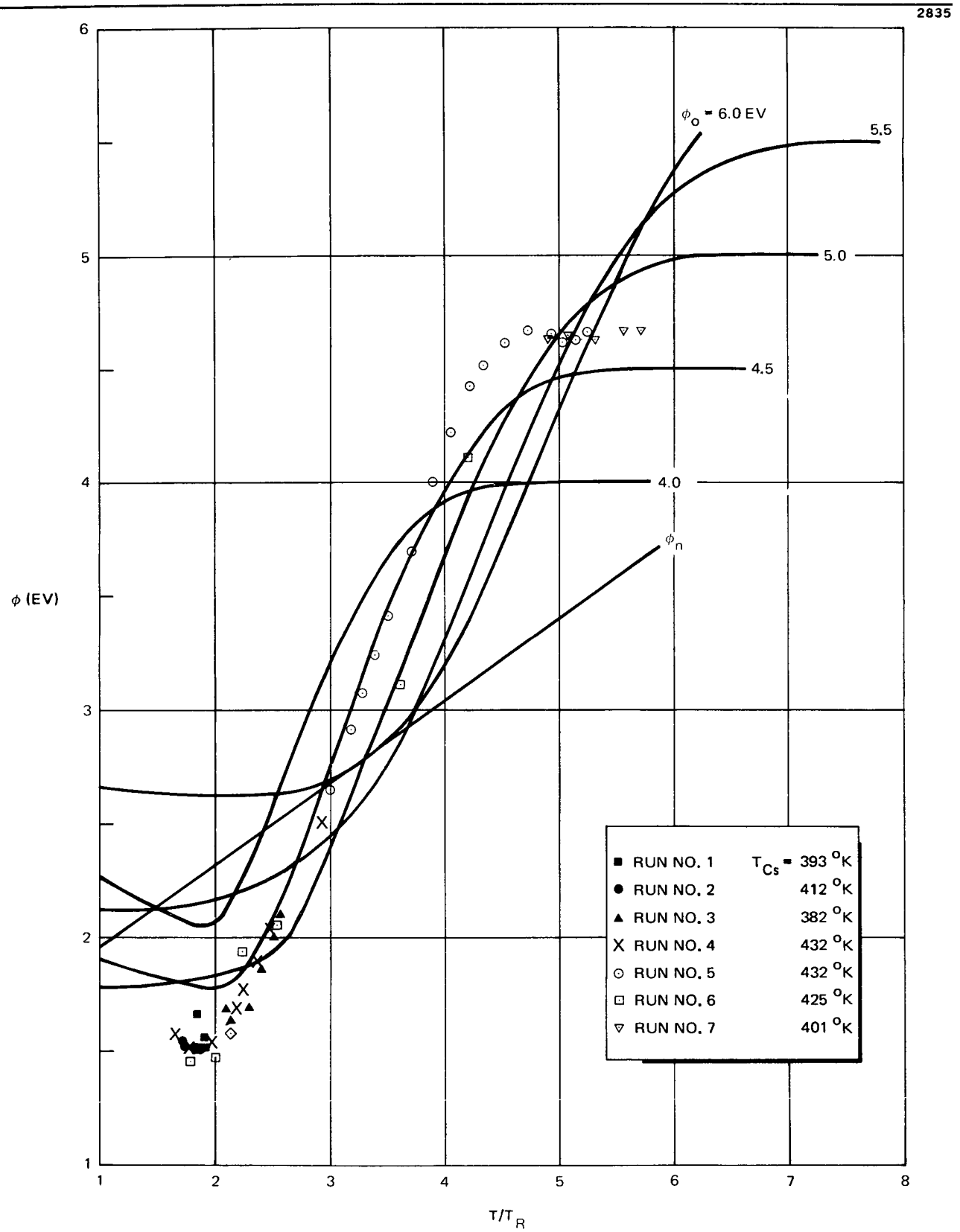

Figure 3-3. ϕ vs T/T_{Cs} Test Emitter No. 2 (10 nm anodic film; ~0.3 a/o oxygen doping)

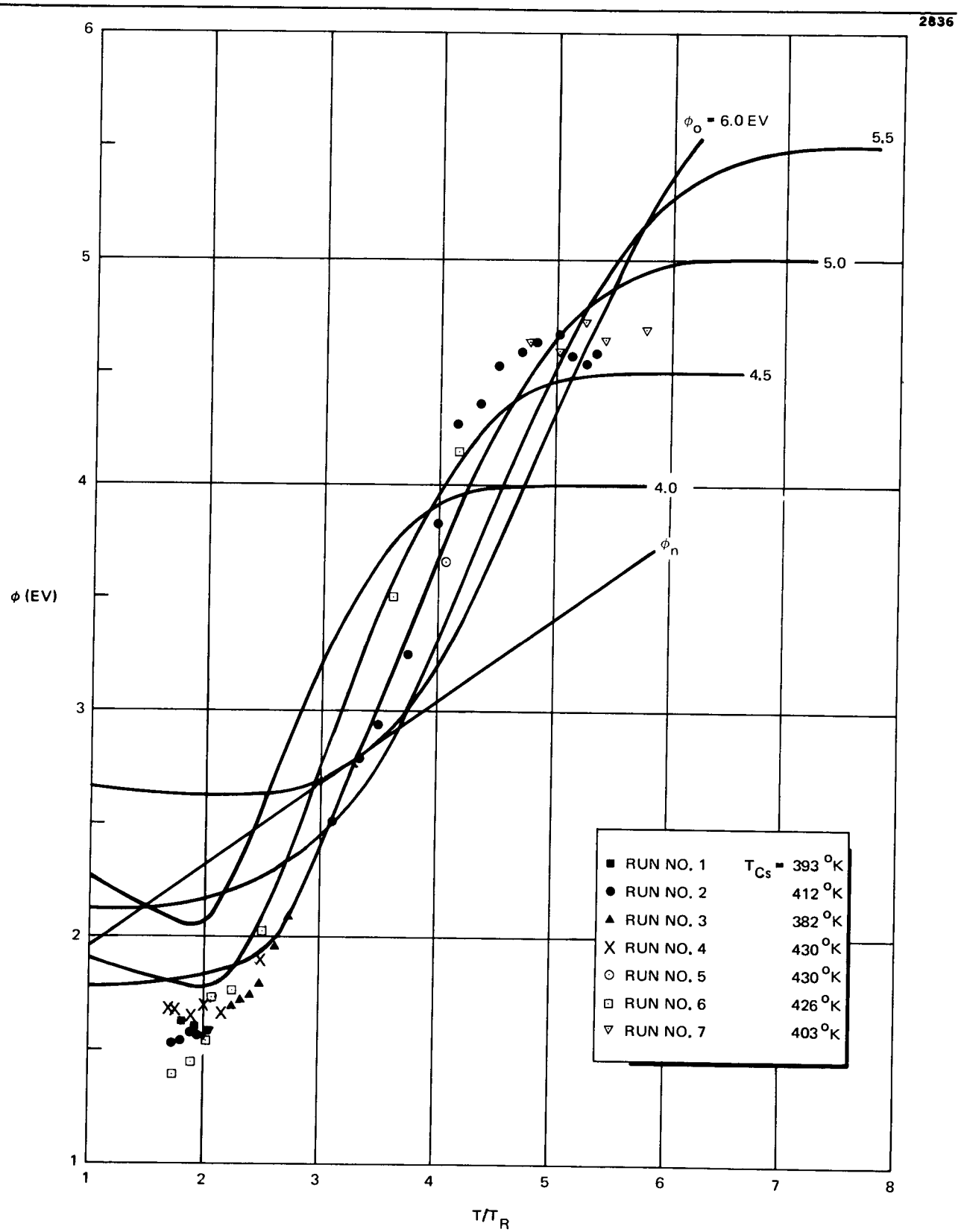

Figure 3-4. ϕ vs T/T_{Cs} Test Emitter No. 3 (118 nm anodic film; ∼0.2 a/o oxygen doping)

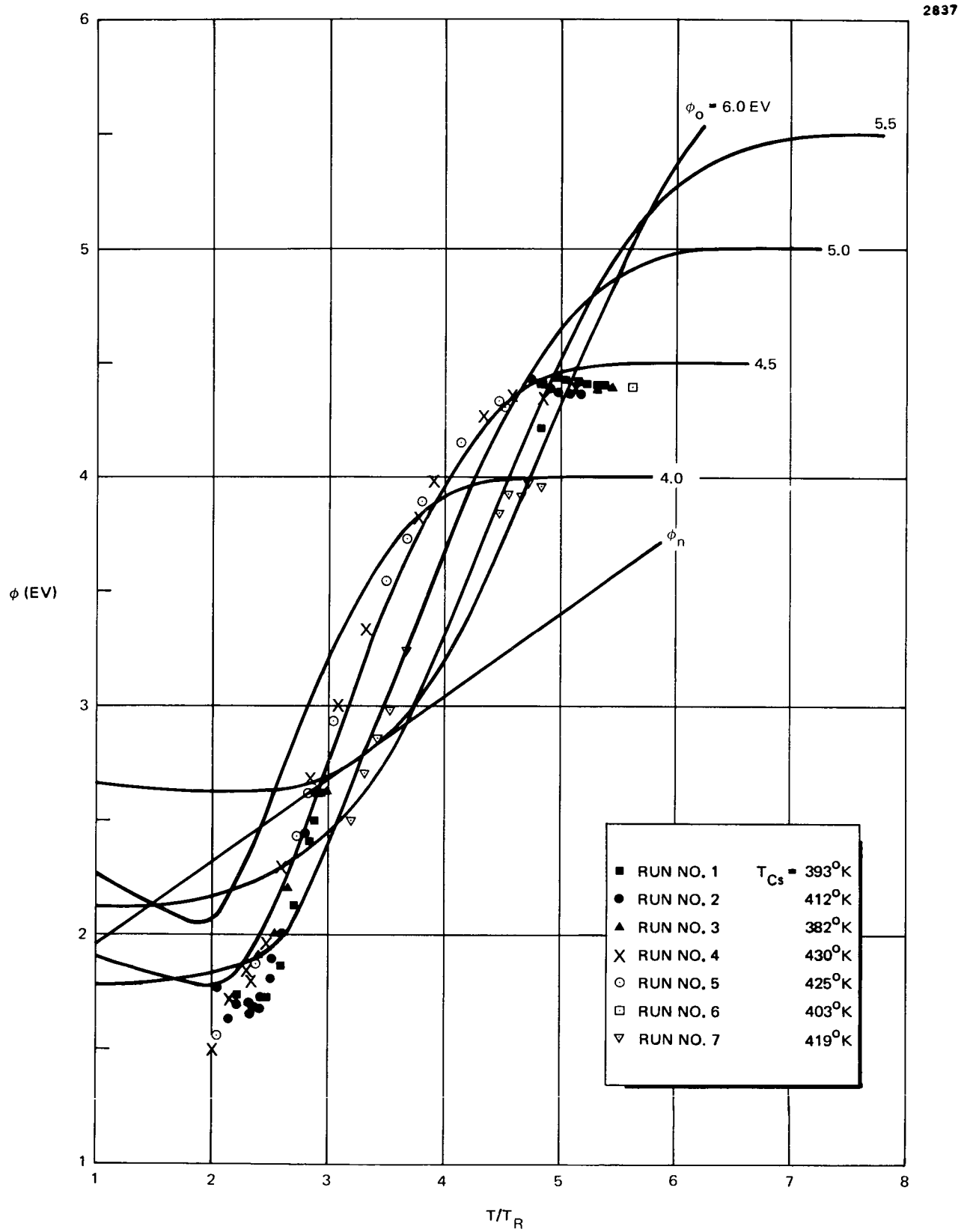

Figure 3-5. ϕ vs T/T_{Cs} Test Emitter No. 4 (tantalum reference electrode)

Discreet structure in the ϕ_{min} region of the anodized-tantalum curves was observed and an unambiguous interpretation of effects is not possible considering contamination from the plasma as indicated by the reference Ta emitter. The data, however, provide interesting qualitative indications. In the range of cesium pressure investigated, the work function minimum appeared to be unaffected by anodic film thickness increasing two orders of magnitude. Emitter No. 3 showed some interesting and distinct structure at a work function of 1.7 ev. The minimum characteristic was much steeper than generally observed below this work function level and showed an discontinuous curve of more conventional shape above 1.7 ev which, in addition, appeared dependent on T_{Cs}. There is qualitative indication of a surface rearrangement at the critical point. Structure of this kind is not apparent in the characteristics of any other test emitter. In general, the shape of minima for anodized specimens is not distinguishable from that of the reference emitter. Any value of the anodic films as a modification to surfaces useful in the collector regime of the conventional plasma diode is obscured by effects which most probably can be attributed to arrival of vapor impurities from the plasma. Intact anodic films with thicknesses to 118 nm as measured optically appeared as normal cesiated surfaces in the Marchuk tube and did not exhibit capacitive effects which might be found in an insulating surface layer.

Emitters 1, 2, and 3 showed a distinct increase in bare work function in the high temperature emitter regime. However, the monotonic dependence on doping level measured in Phase I was not reproduced. The reason for this is probably the loss of oxygen during the time temperature calibrations were performed. The highest indicated bare work function is ~ 4.7 ev contributed by emitter No. 3. The most heavily doped Phase II emitter was emitter No. 2. This indicated a $\phi_0 = 4.66 \pm 0.05$ ev, but this was lower than the characteristic of emitter No. 3 which carried less doping. Emitter 1 containing the lowest doping level also demonstrated an initial plateau at ~ 4.66 ev. On subsequent testing, this decayed to 4.4 ev as oxygen was evaporated from the surface.

None of the anodized and oxygen-doped emitters showed an adsorption regime parallel to the Rasor-Warner Model based on indicated ϕ_0 values. Emitter 1 showed a fair degree of consistency between the plateau and the adsorption region of the characteristic. Emitters 2 and 3 showed scatter which may be

attributed to rapidly changing surface conditions. One data point from emitter No. 2 and three points from No. 3 indicated nonreproducible characteristics corresponding to ϕ_0 ~5.1 ev for the range $3 < T/T_{Cs} < 4$.

Task 6 - Results

In Task 6, the four emitters were heated to 1900° to 1950°K by a common heating current. This was the lowest temperature in the 1700° to 2000°K range which provided a large enough signal to permit discrimination of work function changes. Using the calculated work function as an indication of oxygen doping, the 160-hr test (Figure 3-6) indicated rapid loss of oxygen from the sample with an initial 0.1 a/o doping. Less rapid work function decay was observed with the other doped emitters. The work function of the reference emitter stayed at 4.29 ±0.01 ev during the period. Data corroborated Phase I results by showing a monotonically increasing work function with oxygen doping at the end of the test period. The reservoir effect was demonstrated by the most heavily doped specimen showing the least rapid work function decay. After initial relatively rapid falloff, the rate of work function decay reduced to a gradient which was barely discernable above the resolution power of this measurement technique.

PHASE III RESULTS

Tasks 4 and 5 Experiments

The glass Marchuk tube provided a very low-noise plasma and distinct and reproducible emission traces. Positive ion current levels were reproducible as low as 5 μa.

Work function characteristics of the three test emitters are summarized in Figures 3-7, 3-8, and 3-9. The tungsten reference emitter indicated a generally stable pure tungsten surface with ϕ_0 = 4.60 ±0.05 ev and an adsorption region above ϕ = 3 ev consistent with the bare plateau region. This value is in agreement with literature data. During the experiment, evidence of contamination from the plasma and/or other structures in the tube showed a shift of the lower part of the adsorption region toward the calculated curve corresponding to ϕ_0 = 5 ev. One interesting contrast to this general trend

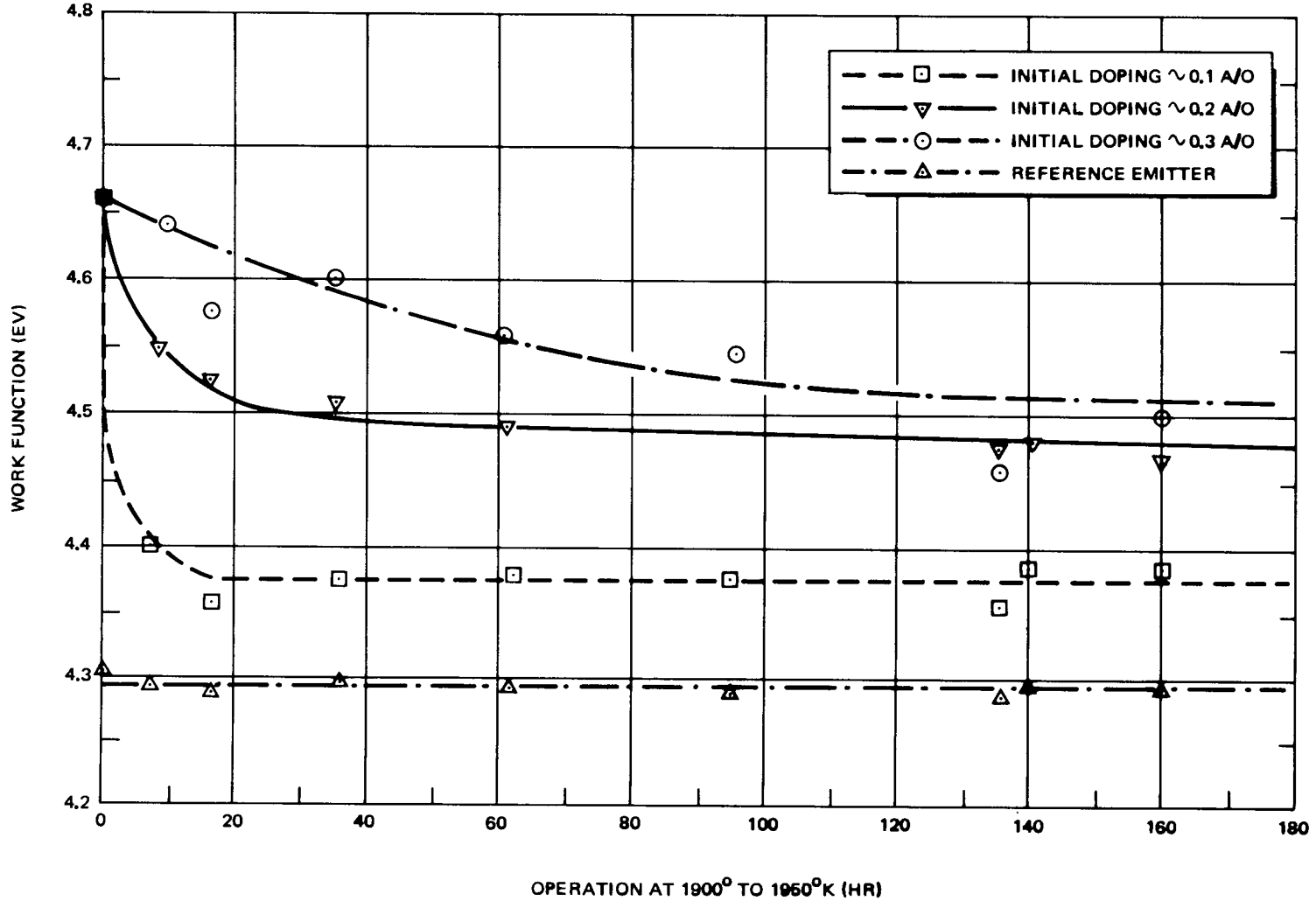

Figure 3-6. Work Function Stability in Temperature Range 1900° to 1950°K

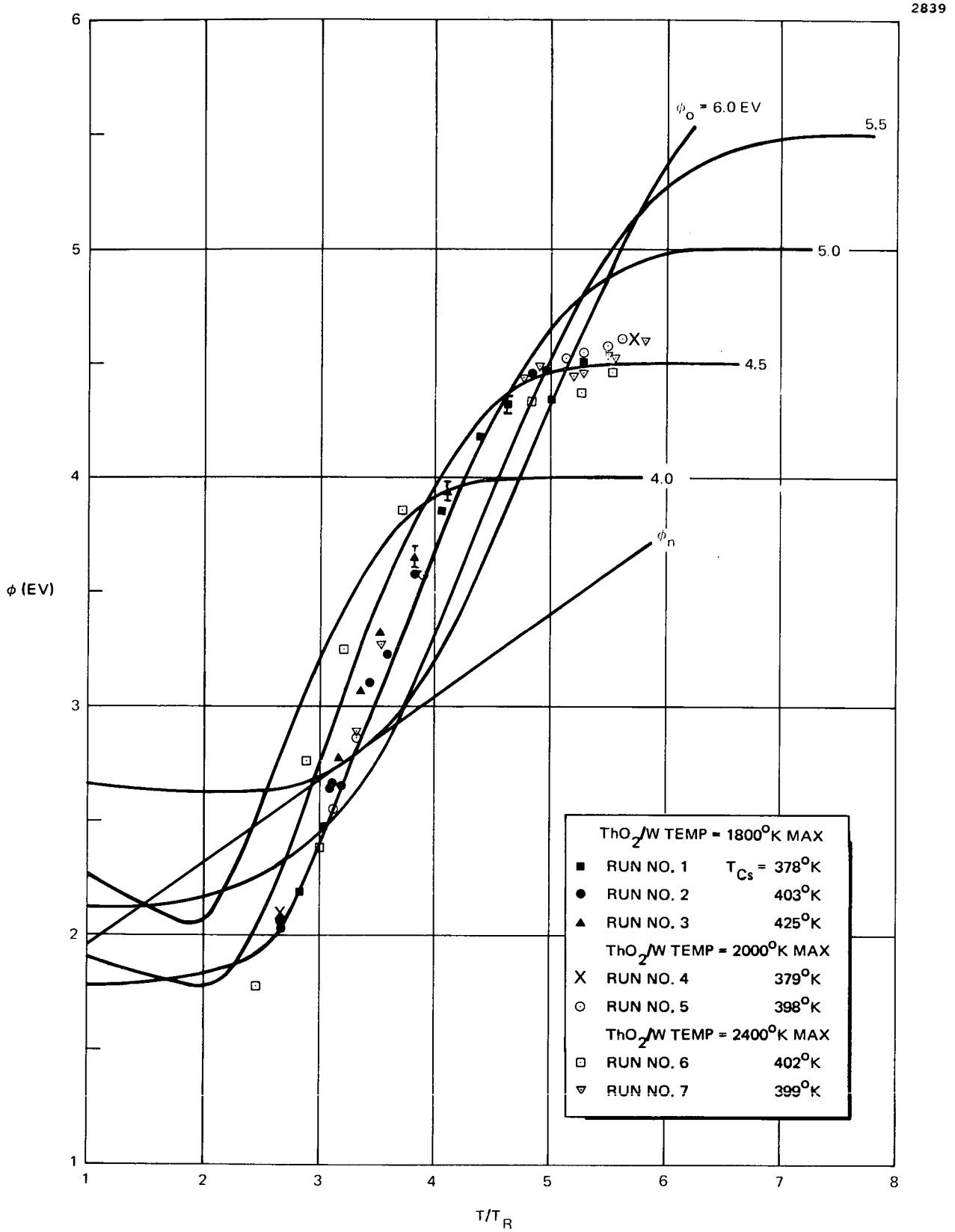

Figure 3-7. ϕ vs T/T$_{Cs}$ Test Emitter No. 1W (W reference)

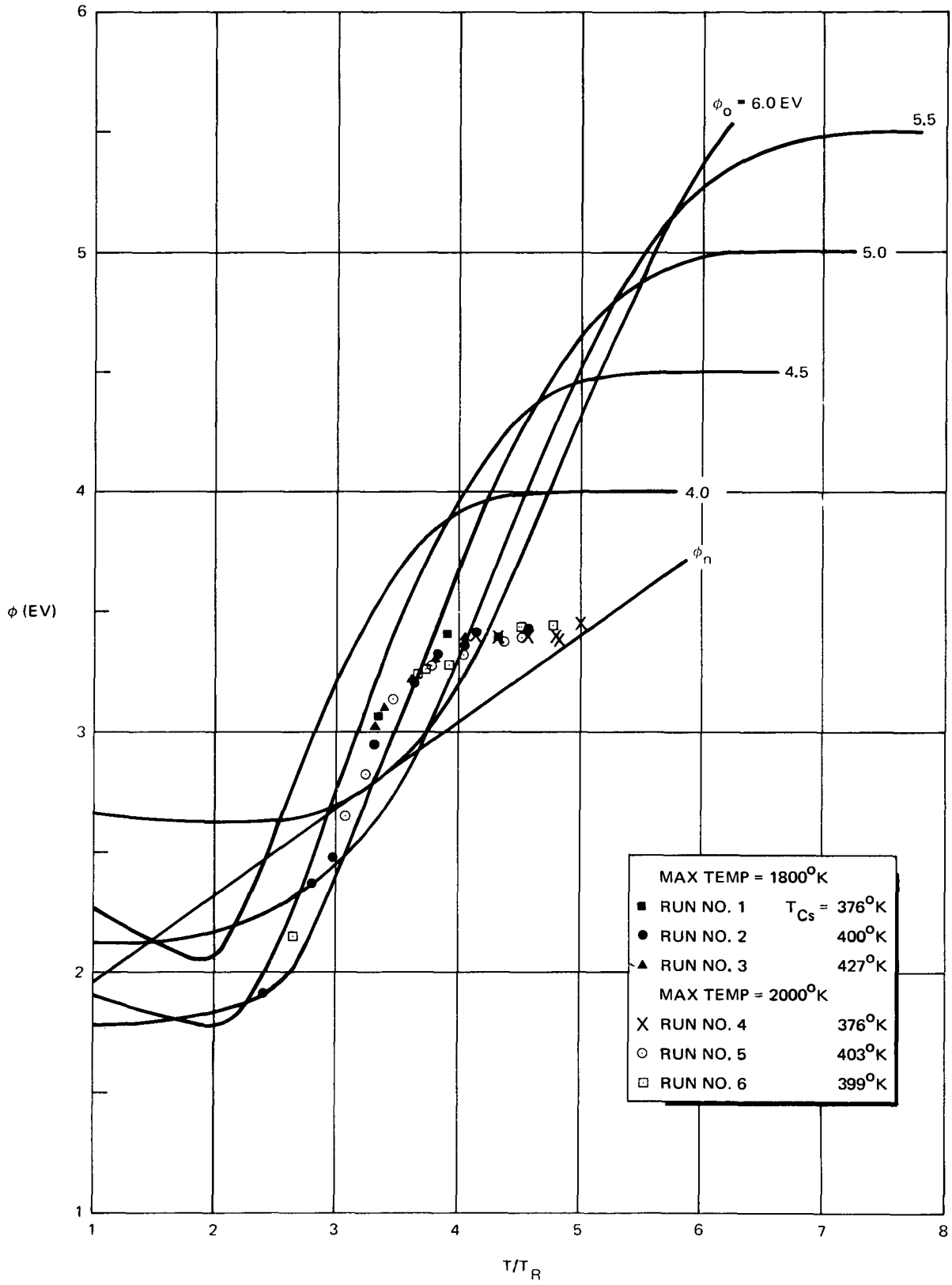

Figure 3-8. ϕ vs T/T_{Cs} Test Emitter No. 2W (ThO_2-W)

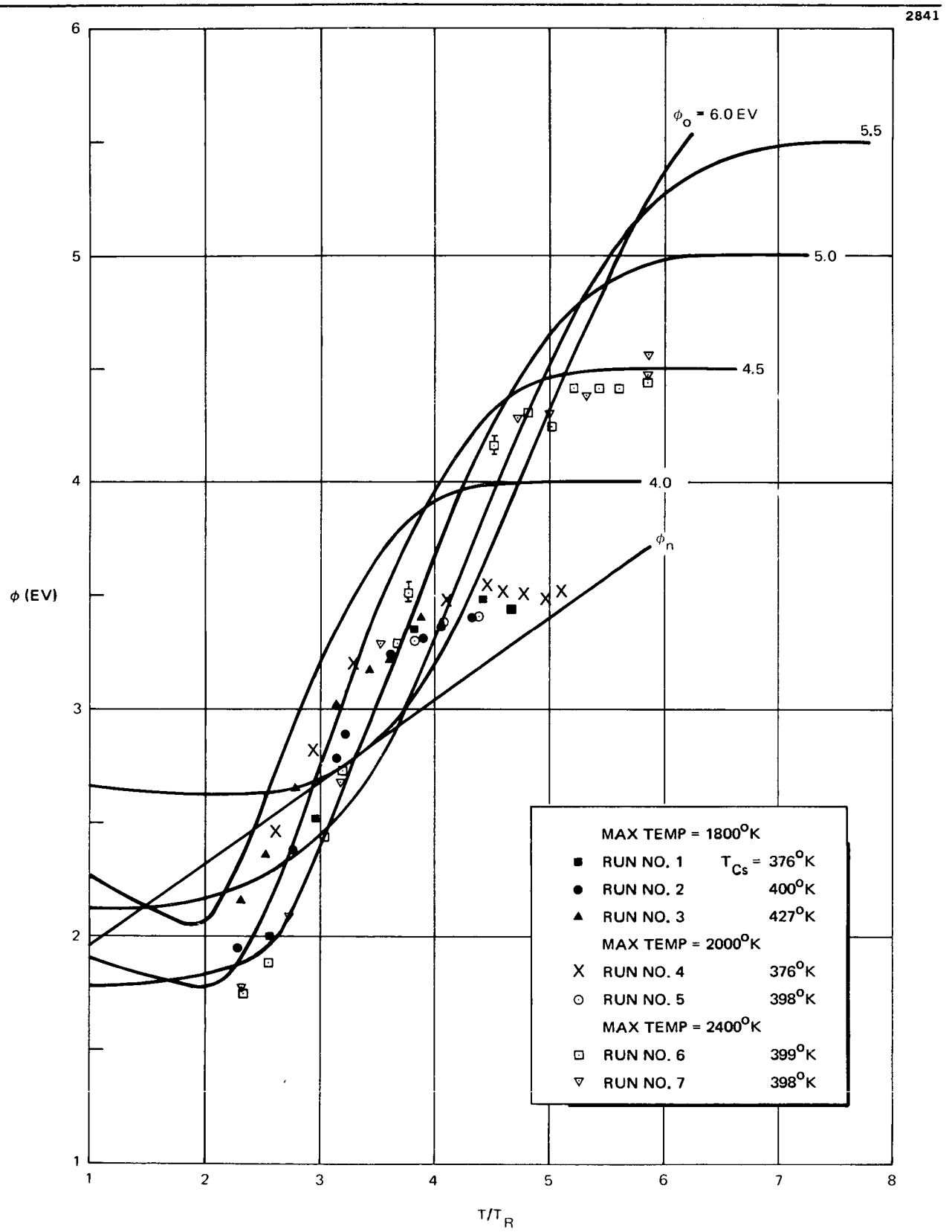

Figure 3-9. ϕ vs T/T_{Cs} Test Emitter No. 3W (ThO_2-W)

was indicated by results of run No. 6 performed after one thoriated-tungsten filament had been operated at 2400°K. A distinct supression of the bare work function plateau to ~4.4 ev and a corresponding shift of the adsorption region to low values of T/T_{Cs} indicated detection and adsorption of an electropositive additive. This was most probably thorium vaporized directly from the adjacent thoriated emitter. The original condition of the tungsten reference emitter was recovered by heating at temperatures to 2400°K, as shown in run No. 7.

Characteristics of test emitter No. 2W shows a plateau at 3.42 ±0.05 ev and correspond very closely to the initial characteristics of emitter No. 3W. The ϕ_0 plateaus agree well with Houston's data for cesiated thorium (Reference 10). Both initial characteristics of thoriated-tungsten emitters merge with the adsorption region expected of a tungsten emitter below ϕ = 3 ev. Characteristics were essentially constant after 1-hr operation at temperatures to 2000°K for each emitter. Test emitter No. 3W was taken incrementally to 2400°K, first to establish a temperature calibration, then to measure thermionic emission. At temperatures above 2000°K, appreciable amounts of thorium appear to have diffused to the surface as indicated by a shift to the left of the ϕ vs T/T_{Cs} diagram as can be expected from the arrival of an electropositive additive. This effect is qualitatively consistent with theoretical expectations. After 1-hr operation at temperatures between 2200° and 2400°K, the source of thorium appeared to be exhausted, and the bare work function characteristic shifted to show a plateau at 4.4 ev. Two hours additional operation at 2400°K shifted the characteristic upward towards that expected for pure tungsten. The final point at 4.57 ev was achieved at the end of run No. 7 after the high temperature exposure. The rate of change of work function in the transition between 4.4 and 4.6 ev was most rapid in the initial minutes of heating. No perceptible change in the bare work function indication was observed after 3 hr of operation at 2400°K. It appears that a work function somewhat less than 4.6 ev is the terminal condition of a depleted thoriated-tungsten emitter.

During high-temperature runs after 2000°K had been reached, there were other indications of the arrival of electronegative additives at the surface in the adsorption regime. A shift to a characteristic corresponding to

$\phi_0 \sim 5$ ev was shown in runs No. 6 and 7. A corresponding shift in the same runs was indicated by the reference tungsten probe which may corroborate the interpretation that oxygen from the depleted thoria was being brought to the surface and vaporized as a tungsten oxide species.

Section 4
CONCLUSIONS

The objectives of the Phase II program were achieved with improved data resolution compared with that in the original Phase I effort. In addition, the Phase II test emitters were successfully prepared to perform as required both in the Phase II program and a rerun of the Phase I effort. The combined Phase I and Phase II programs provided new semiquantitative knowledge of the performance of cesiated tantalum surfaces.

In the emitter regime of cesium plasma converters, the apparent substrate bare work function of tantalum appears to be increased monotonically by oxygen doping within the solid solubility range. Specifically, in the doping range 0.1 to 0.3 a/o the plateau region of the Rasor-Warner curve may be increased to greater than 4.8 ev. In the adsorption regime, a work function of 3 ev may be achieved at $T/T_{Cs} = 3.6$. At the latter point, the surface appears to have a characteristic corresponding to a material with $\phi_0 \sim 5.1$ ev. This treatment decays in less than 150 hours at 1900° to 1950°K. The stability of other doping levels at temperatures 1800°K is a deserving subject for further investigation.

In the collector regime, intact anodic tantalum oxide films on tantalum substrates appear to provide work functions between 1.4 and 1.5 ev at temperatures appropriate for collectors in plasma mode converters. There appears to be structure and indications of surface reorganization within the collector regime; however, the fine structure of these effects was obscured and interpretation compromised by indications of contamination measured by the clean tantalum reference emitter. The results of this work agree semiquantitatively with DWDL experience with similar surfaces prepared for use in low temperature thermionic nuclear batteries (Reference 3). Cesiated anodic films on tantalum substrates, in the range of thickness investigated, showed no characteristics which are distinguishable from metallic electrodes. The absence of capacitive effects and related hysteresis effect in observed emission currents suggested that the character of the cesiated surface was not apparently than of an insulator or semiconductor.

The metal/ceramic Marchuk tube showed no advantage over the conventional glass assembly. The anticipated extension of operating range was not achieved as a result of extreme plasma instability for $T_{Cs} > 470°K$. Spurious discharges were apparent which competed with the main discharge under several conditions in which emission measurements were attempted. The metal/ceramic lead-throughs were susceptible to cesium attack and the demountable electrodes provided no advantage, because significant effort was required to clean tube components for reuse. Despite operation with continuous ion and titanium sublimation pumping, the metal/ceramic tube appeared to generate more contaminating vapors that the conventional sealed-glass configuration. Use of the metal/ceramic Marchuk tube, while useful for inert gas studies, appears, from this experience, quite unsuitable for investigations with cesium vapor. In contrast, the glass Marchuk tube permitted rapid iteration of the experiment and demonstrated higher reliability and lower level of contamination.

Phase III studies generated new knowledge of the performance of thoriated-tungsten emitters in cesium vapor. Of significance, is the indicated bare work function between 3.4 and 3.5 ev which is characteristic of a pure-thorium surface. The transition of the adsorption characteristic to one similar to that of pure tungsten deserves further study, because the thorium density required to indicate a thorium-like plateau, should have remained on the surface to show an electropositive shift in the adsorption region. The terminal condition of depleted thoriated tungsten contrasts with some measurements in related JPL studies. The maximum indicated ϕ_0 in the plateau regime of the Rasor-Warner curve is approximately 4.6 ev, representative of a pure-tungsten sample. This contrasts with $\phi_0 = 5.17$ ev indicated by JPL investigation. The transient appearance of part of the adsorption regime of the curve corresponds to $\phi_0 \sim 5.0$ ev provides the nearest approach to substantiation of the JPL measurements. This effect may be caused by oxygen released from the reduction of thoria diffusing to the surface after the supply of thorium is exhausted. The value of thoriated tungsten in the conventional emitter regime appears to result only after the thorium inventory is depleted. The resulting work function modification is similar to those achieved by techniques involving CVD and/or direct oxidation of tungsten.

Section 5

REFERENCES

1. N.S. Rasor and C. Warner. Correlation of Emission Processes for Adsorbed Alkali Films on Metal Surfaces. J. Appl. Phys. Vol 35, No. 9, 2589, September 1964.
2. J.G. DeSteese. Feasibility Study of Oxygen-Dispensing Emitters for Thermionic Converters Phase I-Final Report, No. MDC G3144 for JPL Contract No. 953125, May 1972.
3. J.G. DeSteese. Development of Thermionic Radioisotope Batteries, MDAC Paper WD-1889 presented to Second International Symposium on Power from Radioisotopes, Madrid, Spain, May 29-June 2, 1972.
4. W.H. Kohl. Handbook of Materials and Techniques for Vacuum Devices. 1967 Edition, Reinhold Publishing Corporation.
5. P.M. Marchuk. Trudy Inst. Fiz. Ak. Nauk. Ukrain 7, 17, 1956.
6. K. Shimada and P.L. Cassell. Plasma-Anode Tube in Metal/Ceramic Envelope. IEEE Record of the 1970 Thermionic Conversion Specialist Conference, Miami Beach, Florida, October 1970.
7. D.A. Vermilyea. The Kinetics of Formation and Structure of Anodic Oxide Films on Tantalum. Acta Metallurgica, 1, 282, 1953.
8. J.G. DeSteese. Influence of Oxygen Doping on the Resistivity of Tantalum, Phase I-Final Report for JPL P.O. No. CA-565932, August 1972.
9. J.G. DeSteese. Influence of Oxygen Doping on the Resistivity of Tantalum, Phase II-Final Report No. DWDL-7210--83 for JPL P.O. No. 565932, October 1972.
10. J.M. Houston. The Thermionic Emission of Hf, Th, and Ti in Cs Vapor, IEEE Record of the 1966 Thermionic Conversion Specialist Conference, Houston, Texas, November 1966.

Appendix A

CERTIFICATION OF TANTALUM WIRE STOCK

The chemical report on annealed tantalum wire 0.01 inch diameter x spool length Production No. W83986 Lot No. MG-87 from Fansteel Inc., Metals Division, is as follows.

Element	Concentration (ppm)
C	10-
O	25
N	25
H	5-
W	100
Cb	270
Zr	10-
Mo	10-
Ti	10-
Fe	10-
Ni	10-
Si	10-
Mn	10-
Ca	10-
Al	10-
Cu	10-
Sn	10-
Cr	10-
V	10-
Mg	10-
Ta	Bal.

Appendix B
CERTIFICATION OF THORIATED TUNGSTEN WIRE STOCK

The chemical report on stress-relieved, cleaned, and straightened 2%-thoriated tungsten wire 0.01-in. diameter x 250 feet, Order No. A-43023 from Thermionics Products Company, is as follows.

Fe	0.02%
Ni	<0.002%
Si	<0.005%
Al	<0.005%
Ca	<0.003%
Mn	<0.003%
Mg	<0.002%
C	0.004%
Mo	0.003%
Thor	2.000%
Tung	97.950%

Appendix C
CHEMICAL ANALYSIS OF TUNGSTEN WIRE STOCK

The results of quantitative spectrographic analysis and gas analysis performed by Ledoux, Inc. on DWDL 0.01 inch diameter tungsten-wire stock used in this program are as follows:

Element	Concentration (ppm)
By Chemical Analysis	
O	105
C	50
H	13
N	6
By Spectrographic Analysis	
Fe	15
Ni	10
W	High

Other elements not detected.